

Flops and Fibrational Geometry of E_7 -models

Mboyo Esole[♣] and Sabrina Pasterski[†]

[♣] Department of Mathematics, Northeastern University
360 Huntington Avenue, Boston, MA 02115, USA
Email: j.esole@northeastern.edu

[†] Princeton Center for Theoretical Science,
Jadwin Hall, Princeton, NJ 08544, USA
Email: sabrina.pasterski@princeton.edu

Abstract:

An E_7 -Weierstrass model is conjectured to have eight distinct crepant resolutions whose flop diagram is a Dynkin diagram of type E_8 . In previous work, we explicitly constructed four distinct resolutions, for which the flop diagram formed a D_4 sub-diagram. The goal of this paper is to explore those properties of a resolved E_7 -model which are not invariant under flops. In particular, we examine the fiber degenerations, identify the fibral divisors up to isomorphism, and study violation of flatness appearing over certain codimension-three loci in the base, where a component of the fiber grows in dimension from a rational curve to a rational surface. For each crepant resolution, we compute the triple intersection polynomial and the linear form induced by the second Chern class, as well as the holomorphic and ordinary Euler characteristics, and the signature of each fibral divisor. We identify the isomorphism classes of the rational surfaces that break the flatness of the fibration. Moreover, we explicitly show that the D_4 flops correspond to the crepant resolutions of the orbifold given by \mathbb{C}^3 quotiented by the Klein four-group.

Keywords: Elliptic fibrations, Crepant morphisms, Resolution of singularities, Weierstrass models

Contents

1	Introduction and summary	2
2	Preliminaries	4
2.1	Defining the E_7 -model	4
2.2	Root system of E_7 and the weights of its fundamental representation 56	5
2.3	Chamber structure of the hyperplane $I(E_7, \mathbf{56})$	7
3	Fiber degenerations of an E_7-model	10
4	D_4-flops of the E_7-model as flops of the orbifold $\mathbb{C}^3/(\mathbb{Z}_2 \times \mathbb{Z}_2)$	14
5	Triple intersection numbers	16
6	Isomorphism classes of fibral divisors	19
7	Characteristic numbers of fibral divisors	21
8	Fat fibers and loss of flatness	24
A	Fiber degenerations	27
A.1	Ch_1	27
A.2	Ch_2	28
A.3	Ch_3	30
A.4	Ch_4	31
A.5	Ch_5	32
A.6	Ch_6	33
A.7	Ch_7	35
A.8	Ch_8	36
B	Triple intersection computations	37
B.1	Y_4	37
B.2	Y_5	38
B.3	Y_6	40
B.4	Y_8	41
C	Fibral divisors from scaling	44
D	Vertical rational surfaces	44
D.1	The vertical surface Q_8	45
D.2	The vertical surface Q_6	46
D.3	The vertical surface Q_5	47
D.4	The vertical surface Q_4	48

1 Introduction and summary

The study of crepant resolutions of singular Weierstrass models lies at the crossroads of algebraic geometry, number theory, and string theory. In mathematics, interest in elliptic fibrations started with the pioneering work of Kodaira, Néron, Tate, Deligne, and others. Ever since, elliptic fibrations have appeared in a variety of situations from algebraic geometry to number theory. In Calabi–Yau compactifications, elliptic fibrations are ubiquitous, as a large majority of known Calabi–Yau varieties are elliptically fibered. These hold a special place in birational geometry. Meanwhile elliptic fibrations play a key role in M-theory and F-theory compactifications. In both F-theory and M-theory, elliptic fibrations offer elegant geometrizations of aspects of supersymmetric gauge theories. In particular, elliptically fibrations are at the heart of the constructions of new super-conformal field theories that often have no alternative description. The extended Kähler cones of Calabi–Yau threefolds are closely related to the Coulomb phases of five-dimensional supersymmetric gauge theories with eight supersymmetric charges.

Simple types of elliptic fibrations are the so called G -models where G is a simply connected compact Lie group associated with a Kodaira fiber whose dual graph is the affine version of the Dynkin diagram of the Lie algebra \mathfrak{g} of G . Among the G -models with G a compact exceptional Lie group, those not fully well understood are E_6 and E_7 , since they are the only ones allowing flops. Unfortunately, not all possible minimal models corresponding to a Weierstrass model of type E_6 and E_7 are known explicitly. An E_7 -model is conjectured to have eight distinct crepant resolutions whose flop diagram is a Dynkin diagram of type E_8 (see Figure 4). Any two crepant resolutions of the same variety are related by a finite sequence of flops and have the same Euler characteristic and Hodge numbers.¹ The goal of this paper is to explore those properties of a resolved E_7 -model which are not invariant under flops. Examples include the geometry of its fibral divisors as well as its intersection ring and the geometry of its fat fibers. The key results of this paper are as follows:

- a) *Fiber degenerations of an E_7 -model* (see Table 1)

We study degenerations of the generic curve of the fibral divisors using the hyperplane arrangement I(**56**, E_7). In this way, we avoid the box graph method used in [27] and correct a few discrepancies in the literature [6, 11, 12, 25, 27]. In particular, for the chamber where the affine node can degenerate, we identify the correct splitting which was missing in [12] and inaccurate in [11, 27]. We regard this result as a completion of the work of Diaconescu and Entin [12].

- b) *D_4 -flops of the E_7 -model as flops of the orbifold $\mathbb{C}^3/(\mathbb{Z}_2 \times \mathbb{Z}_2)$* (see Figure 7)

In [25], we explicitly constructed four of the eight conjectured E_7 minimal models and showed that their flops define a Dynkin diagram of type D_4 . We now give a direct answer to a question raised in that paper. Namely, we show that the flops between the minimal models Y_4 , Y_5 , Y_6 , and Y_8 correspond to flops between the four crepant resolutions of the orbifold $\mathbb{C}^3/(\mathbb{Z}_2 \times \mathbb{Z}_2)$, which is isomorphic to the binomial variety

$$\mathbb{C}[u_1, u_2, u_3, t]/(t^2 - u_1 u_2 u_3).$$

¹The generating function for the Euler characteristic of G -models, as well as the Hodge numbers for the Calabi–Yau threefold case can be found in [18]. Additional characteristic invariants preserved by flops are given in [20].

c) *Triple intersection numbers* (see Theorem 5.9)

We compute the triple intersection polynomial of the fibral divisors in all chambers for which we have an explicit crepant resolution of the singularities

$$F_m(\phi) = \int_{Y_m} \left(\sum_{a=0}^7 D_a \phi_a \right)^3, \quad m = 4, 5, 6, 8.$$

The triple intersection depends on the chamber but not the blowups used to reach it. This data is useful for determining the matter representations which appear in F -theory compactifications. We consider specializations to the case of Calabi-Yau manifolds, and further to $S^2 = -8$ and $g = 0$, relevant to the CFT literature.

d) *Isomorphism classes of fibral divisors* (see Table 3, Section 6)

We identify the fibral divisors of an E_7 -model up to isomorphism by exploiting the known crepant resolutions. In doing so, we also learn something about those chambers for which we do not have an explicit geometric construction. When two chambers are connected by a flop that does not change D_i , the isomorphism class of D_i remains the same. This implies that we can easily move from chamber to chamber by flops and learn about the fiber geometry (modulo some empty entries).

e) *Characteristic numbers of fibral divisors* (see Theorems 7.1 and 7.3)

We give the linear functions induced on $H^2(Y, \mathbb{Z})$ by the second Chern class of the minimal models $Y = \{Y_4, Y_5, Y_6, Y_8\}$

$$\mu : H^2(Y, \mathbb{Z}) \rightarrow \mathbb{Z} \quad D \mapsto \int_Y D \cdot c_2(TY)$$

as well as characteristic numbers of the fibral divisors D_a for each of these varieties. In particular, we consider the signature $\tau(D)$ as well as the holomorphic $\chi_0(D)$ and ordinary $\chi(D)$ Euler characteristics. These characteristic numbers provide precious information about the structure of the fibral divisors. For instance, the signature and the Euler characteristic also give information on the number of charged hypermultiplets and the number of rational curves appearing when the E_7 fibers degenerate.

f) *Fat fibers and loss of flatness* (see Figure 8)

In each minimal model Y_a we analyze, the generic fiber C_6 of the fibral divisor D_6 specializes to a rational surface Q_a over a codimension-three locus in the base, and does not give a flat fibration. The rational surfaces Q_8 and Q_6 are isomorphic to the Hirzebruch surfaces \mathbb{F}_2 and \mathbb{F}_1 , respectively, and are related by the usual Nagata transformation with Q_5 serving as the intermediate surface. The rational surface Q_5 is obtained by blowing-up a point of the (-1) -curve of $Q_6 \cong \mathbb{F}_1$ or by blowing-up a point of the curve of self-intersection 2 in $Q_8 \cong \mathbb{F}_2$. The rational surface Q_4 is obtained by blowing-up the intersection of the two (-1) -curves of Q_5 .

This paper is organized as follows. We spend Section 2 reviewing the necessarily preliminaries. We then present results a)-f) summarized above in sections 3-8, respectively.

2 Preliminaries

In this section, we introduce the E_7 Weierstrass model, give our conventions for the Dynkin diagrams of E_7 and E_8 , write out the weights for the fundamental representation **56** of E_7 , and review the structure of the hyperplane arrangement $I(E_7, \mathbf{56})$ as analyzed in [25].

2.1 Defining the E_7 -model

Consider a smooth variety B , a line bundle $\mathcal{L} \rightarrow B$, and define the projective bundle

$$\pi : X_0 = \mathbb{P}_B[\mathcal{O}_B \oplus \mathcal{L}^{\otimes 2} \oplus \mathcal{L}^{\otimes 3}] \rightarrow B.$$

A Weierstrass model is the zero scheme of a section of the bundle² $\mathcal{O}_{X_0}(3) \otimes \pi^* \mathcal{L}^{\otimes 6}$. We can make this more explicit by denoting the relative projective coordinates of X_0 as $[z : x : y]$. Then a Weierstrass model can be written as the vanishing locus³

$$V(y^2z - x^3 - fxz^2 - gz^3), \quad (2.1)$$

where f is a section of $\mathcal{L}^{\otimes 4}$ and g is a section of $\mathcal{L}^{\otimes 6}$. The discriminant and the j -invariant are

$$\Delta = 4f^3 + 27g^2, \quad j = 1728 \frac{4f^3}{\Delta}.$$

The discriminant locus $V(\Delta)$ consists of points in B over which the fiber is singular.

Let B be a smooth variety and $S = V(s)$ be a smooth prime divisor in B given by the zero locus of a section s of a line bundle \mathcal{S} . An E_7 -model is given by a Weierstrass model such that (see Proposition 4 of [36] and Step 9 of Tate's algorithm)

$$y^2z = x^3 + as^3xz^2 + bs^5z^3, \quad (2.2)$$

where a is a section of $\mathcal{L}^{\otimes 4} \otimes \mathcal{S}^{-\otimes 3}$, and b is a section of $\mathcal{L}^{\otimes 6} \otimes \mathcal{S}^{-\otimes 5}$. Moreover, we assume that a and b have zero valuation along S and $V(a)$ and $V(b)$ are smooth divisors in B which intersect transversally. For this model the discriminant

$$\Delta = s^9(4a^3 + 27b^2s) \quad (2.3)$$

factorizes into components S and $\Delta' = V(4a^3 + 27b^2s)$. The generic fiber over S is of Kodaira type III* and that over Δ' is of type I₁. The divisor Δ' has cuspidal singularities at $V(a, b)$ which worsen to triple point singularities over $V(a, b, s)$. S and Δ' do not intersect transversally, but rather at the triple points (s, a^3) . At the support of this intersection, we have the following degeneration:

$$\Delta' \cap S = V(s, a) : \quad \text{III}^* + \text{I}_1 \rightarrow \text{II}^*. \quad (2.4)$$

²Here $\mathcal{O}_{X_0}(1)$ is the dual of the tautological line bundle of X_0 .

³Given a set of line bundles \mathcal{L}_i with sections f_i we denote their zero scheme $f_1 = f_2 = \dots = f_r = 0$ as $V(f_1, \dots, f_r)$.

2.2 Root system of E_7 and the weights of its fundamental representation **56**

The Lie algebra of type E_7 has dimension 133, and Weyl group of order $2^{10} \cdot 3^4 \cdot 5 \cdot 7$ [9, Plate VI]. The Cartan matrix of E_7 is

$$\begin{matrix} \alpha_1 \\ \alpha_2 \\ \alpha_3 \\ \alpha_4 \\ \alpha_5 \\ \alpha_6 \\ \alpha_7 \end{matrix} \begin{pmatrix} 2 & -1 & 0 & 0 & 0 & 0 & 0 \\ -1 & 2 & -1 & 0 & 0 & 0 & 0 \\ 0 & -1 & 2 & -1 & 0 & 0 & -1 \\ 0 & 0 & -1 & 2 & -1 & 0 & 0 \\ 0 & 0 & 0 & -1 & 2 & -1 & 0 \\ 0 & 0 & 0 & 0 & -1 & 2 & 0 \\ 0 & 0 & -1 & 0 & 0 & 0 & 2 \end{pmatrix} \quad (2.5)$$

where the i th row gives the coordinates of the simple root α_i in the basis of fundamental weights. As compared to Bourbaki's tables, our $(\alpha_1, \alpha_2, \alpha_3, \alpha_4, \alpha_5, \alpha_6, \alpha_7)$ are denoted $(\alpha_1, \alpha_3, \alpha_4, \alpha_5, \alpha_6, \alpha_7, \alpha_2)$, respectively.

The affine Dynkin diagrams for \tilde{E}_7 and \tilde{E}_8 are provided in Figure 1 and Figure 2, respectively. The Hasse diagram for the representation **56** of E_7 is given in Figure 3. The affine Dynkin diagram of type \tilde{E}_7 appears as the dual graph of the generic fiber over S for the E_7 -model.

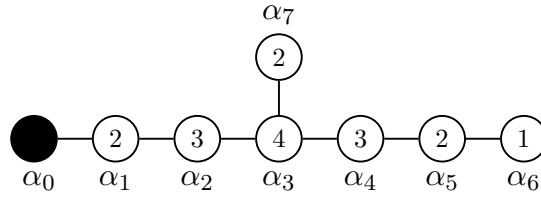


Figure 1: Affine Dynkin diagram of type \tilde{E}_7 , which reduces to the Dynkin diagram of type E_7 when the black node is removed. The numbers inside the nodes are the multiplicities of the Kodaira fiber of type III^* and the Dynkin labels of the highest root. The root α_1 is the highest weight of the adjoint representation while α_6 is the highest weight of the fundamental representation **56**.

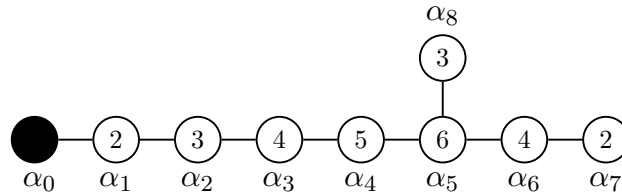


Figure 2: Affine Dynkin diagram of type \tilde{E}_8 , which reduces to the Dynkin diagram of type E_8 when the black node is removed. The numbers in the nodes are the multiplicities of the Kodaira fiber of type II^* .

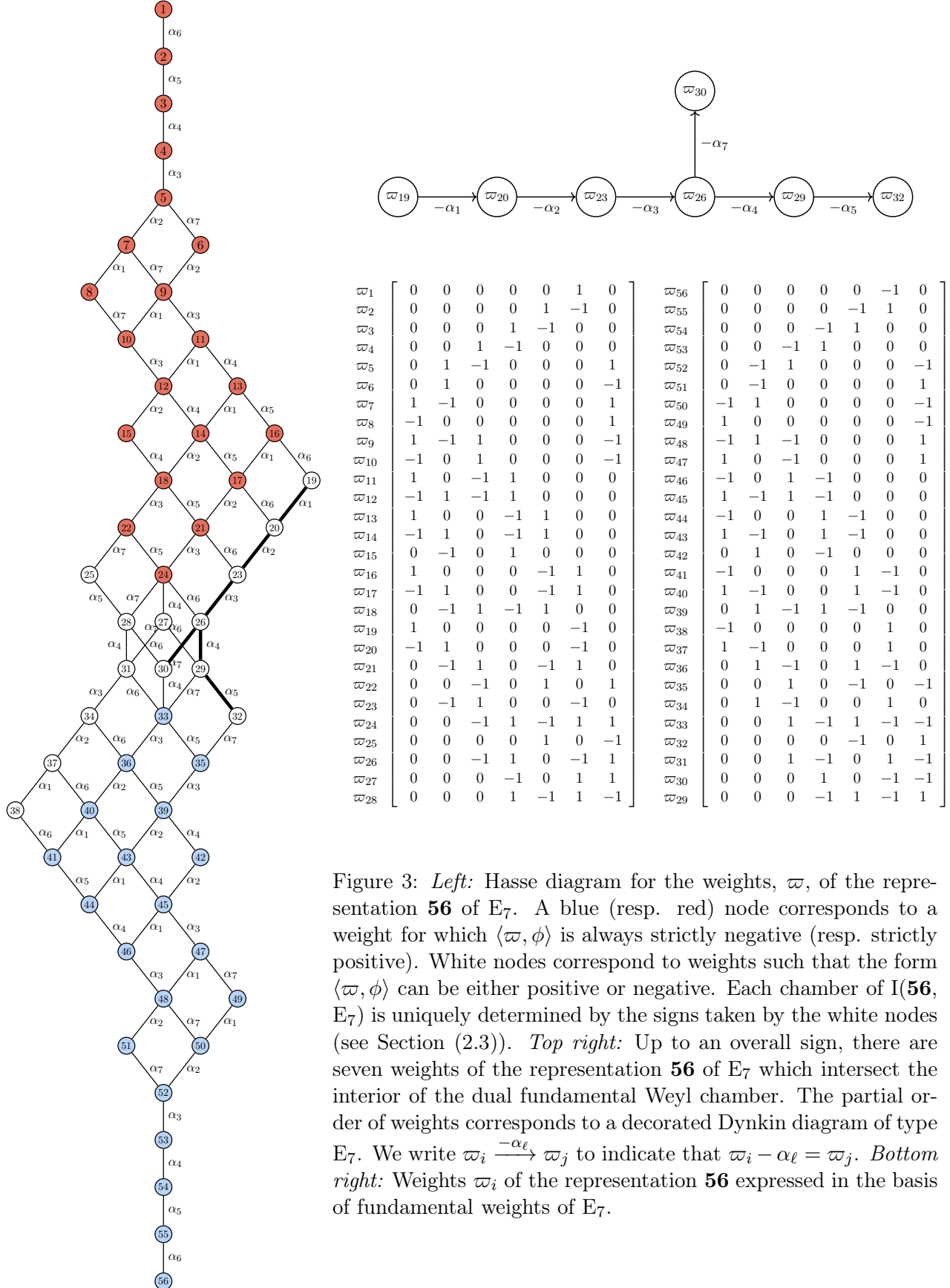


Figure 3: *Left*: Hasse diagram for the weights, w , of the representation **56** of E_7 . A blue (resp. red) node corresponds to a weight for which $\langle w, \phi \rangle$ is always strictly negative (resp. strictly positive). White nodes correspond to weights such that the form $\langle w, \phi \rangle$ can be either positive or negative. Each chamber of $I(\mathbf{56}, E_7)$ is uniquely determined by the signs taken by the white nodes (see Section (2.3)). *Top right*: Up to an overall sign, there are seven weights of the representation **56** of E_7 which intersect the interior of the dual fundamental Weyl chamber. The partial order of weights corresponds to a decorated Dynkin diagram of type E_7 . We write $w_i \xrightarrow{-\alpha_\ell} w_j$ to indicate that $w_i - \alpha_\ell = w_j$. *Bottom right*: Weights w_i of the representation **56** expressed in the basis of fundamental weights of E_7 .

2.3 Chamber structure of the hyperplane $I(E_7, \mathbf{56})$

In this section, we review the structure of the hyperplane arrangement $I(E_7, \mathbf{56})$, following the presentation of [25].

Definition 2.1. For a choice of positive simple roots α_i , the *open dual fundamental Weyl chamber* is the cone of coroots ϕ such that: $\langle \alpha_i, \phi \rangle > 0$ for $i = 1, \dots, r$.

Given a Lie algebra \mathfrak{g} of rank r and a representation \mathbf{R} of \mathfrak{g} , the set of weights of \mathbf{R} is a poset with the usual ordering relation:

$$\varpi_a \preceq \varpi_b \iff \varpi_a - \varpi_b \text{ is a sum of positive roots.}$$

The kernel of a weight ϖ is the hyperplane $\varpi^\perp := \{\phi \mid \langle \varpi, \phi \rangle = 0\}$ in the space of coroots.

Definition 2.2. A weight ϖ of representation \mathbf{R} is *extremal* if the hyperplane ϖ^\perp intersects the interior of the dual fundamental Weyl chamber of \mathfrak{g} .

If we restrict the ambient space to the open dual fundamental Weyl chamber, the only weights giving hyperplanes which intersect this space are the extremal weights, by definition. The correspondence between weights and perpendicular hyperplanes is not one-to-one so long as two weights can be parallel. We therefore make a choice of extremal weight for each hyperplane, fix an order $(\varpi_1, \dots, \varpi_q)$, and define a *sign vector* $v(\phi)$ whose k th entry is

$$v_k(\phi) = \text{Sign}(\langle \varpi_k, \phi \rangle) \quad \text{where} \quad \text{Sign}(x) = \begin{cases} -1 & \text{if } x < 0 \\ 0 & \text{if } x = 0 \\ 1 & \text{if } x > 0. \end{cases}$$

A simple way to tell if a weight is extremal is to write it in the basis of simple roots and use the following theorem.

Theorem 2.3. *A weight is extremal if and only if at least two of its coefficients in the basis of simple roots have different signs.*

Definition 2.4. An *open chamber* of the hyperplane arrangement $I(\mathfrak{g}, \mathbf{R})$ is a connected component of the dual open Weyl chamber minus the union of the hyperplanes ϖ_m^\perp .

Each open chamber is uniquely determined by the entries of the sign vector, which take the values ± 1 , and are constant within each open chamber.

In particular, the partial order for the weights that are interior walls is (see Figure 3):

$$\varpi_{19} \succ \varpi_{20} \succ \varpi_{23} \succ \varpi_{26} \succ \varpi_{29} \succ \varpi_{32}, \quad \varpi_{26} \succ \varpi_{30}. \quad (2.6)$$

Our choice of sign vector for the hyperplane arrangement $I(E_7, \mathbf{56})$ is as follows:⁴

$$\phi \mapsto (\langle \varpi_{19}, \phi \rangle, \langle \varpi_{20}, \phi \rangle, \langle \varpi_{23}, \phi \rangle, \langle \varpi_{26}, \phi \rangle, \langle \varpi_{29}, \phi \rangle, \langle \varpi_{32}, \phi \rangle, \langle \varpi_{30}, \phi \rangle), \quad (2.7)$$

⁴Each weight of the representation $\mathbf{56}$ has norm square $3/2$ and has scalar product $\pm 1/2$ with any other weight of $\mathbf{56}$. Our choice of signs for the entries of the sign vector is such that the highest weight $\boxed{0 \ 0 \ 0 \ 0 \ 1 \ 0}$ has a sign $(-1, -1, -1, -1, -1, -1, -1)$.

which expands to

$$v(\phi) = \text{Sign}(\phi_1 - \phi_6, -\phi_1 + \phi_2 - \phi_6, -\phi_2 + \phi_3 - \phi_6, \\ -\phi_3 + \phi_4 - \phi_6 + \phi_7, -\phi_4 + \phi_5 - \phi_6 + \phi_7, -\phi_5 + \phi_7, \phi_4 - \phi_6 - \phi_7). \quad (2.8)$$

Definition 2.5. Two chambers Π_1 and Π_2 are said to be *incident* if they share a common wall ϖ_k^\perp , in which case their sign vectors differ only in their k^{th} component.

The incidence matrix of the chambers has a dual graph which gives the geography of chambers of the hyperplane arrangement $I(\mathfrak{g}, \mathbf{R})$. The incidence graph for the hyperplane arrangement $I(E_7, \mathbf{56})$ is given in Figure 4.

Theorem 2.6. *The hyperplane arrangement $I(E_7, \mathbf{56})$ has eight chambers, each of which is simplicial. The adjacency graph of the chambers is isomorphic to the Dynkin diagram of type E_8 .*

Explicitly our sign vector in equation (2.7) obeys the following rules:

1. The negative sign flows as the arrows of Figure 3.
2. The forms $\langle \varpi_{30}, \phi \rangle$ and $\langle \varpi_{29}, \phi \rangle$ cannot both be positive at the same time.

For example, if $\langle \varpi_{19}, \phi \rangle$ is negative, the same is true of all the $\langle \varpi_i, \phi \rangle$ with $i = \{20, 23, 26, 29, 32, 30\}$. The second rule arises from the fact that $\varpi_{30} + \varpi_{29} = -\alpha_6$ and $\langle \alpha_6, \phi \rangle > 0$, since we are restricted to the interior of the dual fundamental Weyl chamber. To define a chamber, we just need to name which one of the $\langle \varpi_i, \phi \rangle$ is the first negative one with respect to the order given above. For the case where both $\langle \varpi_{26}, \phi \rangle$ and $\langle \varpi_{30}, \phi \rangle$ are positive, then $\langle \varpi_{19}, \phi \rangle$, $\langle \varpi_{20}, \phi \rangle$, and $\langle \varpi_{23}, \phi \rangle$ are all positive. Since $\langle \varpi_{30}, \phi \rangle$ is positive, $\langle \varpi_{29}, \phi \rangle$ is necessarily negative, which forces $\langle \varpi_{32}, \phi \rangle$ to also be negative. There are exactly eight possibilities satisfying these two rules. They are listed in Figure 5.

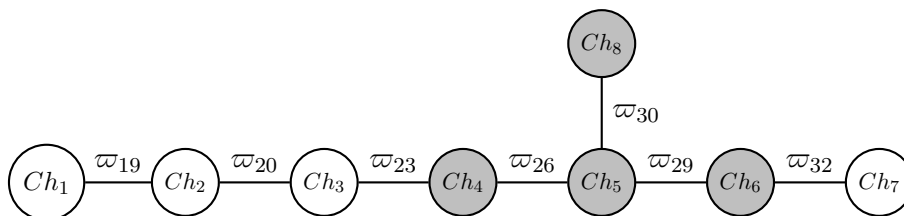


Figure 4: Incidence graph of the chambers of the hyperplane arrangement $I(E_7, \mathbf{56})$. A weight ϖ between two nodes indicates that the corresponding chambers are separated by the hyperplane ϖ^\perp : for example, one goes from Ch_1 to Ch_2 by crossing the hyperplane ϖ_{19}^\perp . The colored chambers forming a subgraph of type D_4 are those corresponding to the nef-cone of the crepant resolutions constructed by explicit blowups in [25].

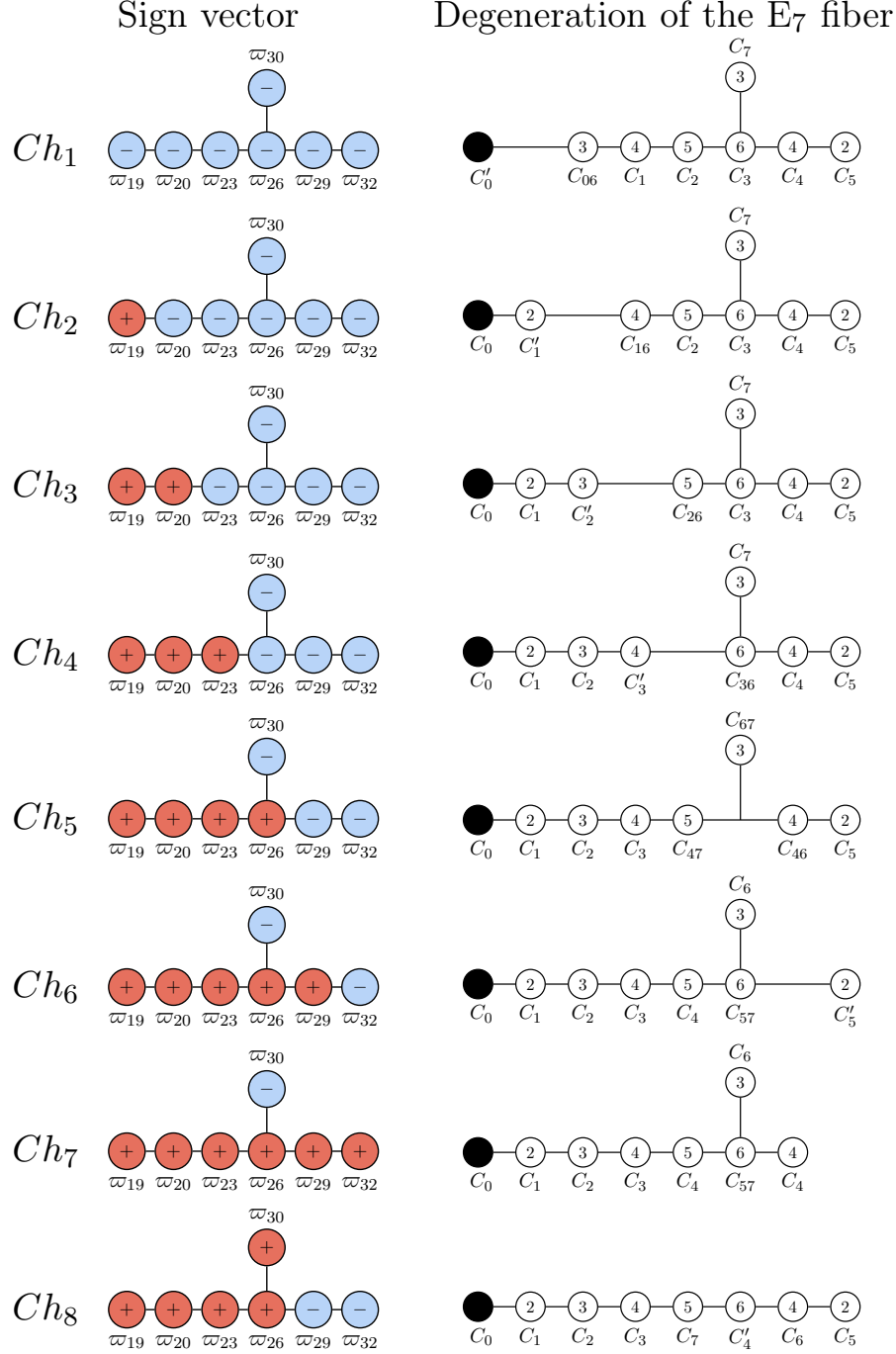


Figure 5: The eight chambers of $I(E_7, \mathbf{56})$. Each chamber is uniquely defined by the signs taken by the seven linear functions $\langle \varpi_i, \phi \rangle$ for $i = \{19, 20, 23, 26, 29, 32, 30\}$, which together define a sign vector for the hyperplane arrangement. The left column gives the entries of the sign vector for each chamber. The right column gives the singular fibers observed or expected over $V(s, a)$. In Chamber i , the singular fiber over $V(s, a)$ is expected to have as a dual graph the affine E_8 Dynkin diagram with the node i contracted to a point [27]. The singular fibers are observed directly in an explicit crepant resolution in chambers 4,5,6,8 in [25] and need to be confirmed geometrically in Chambers 1, 2, 3, and 7.

3 Fiber degenerations of an E_7 -model

Figure 5 also summarizes the structure of the singular fiber over $V(s, a)$ in each chamber. In this section, we explore this degeneration of the fiber III^* (with dual graph the affine E_7 Dynkin diagram) to an incomplete II^* (with dual graph E_8). We begin with the physical motivation for this computation, as well as a few more definitions needed to explain our strategy.

In a five-dimensional supersymmetric gauge theory with gauge algebra \mathfrak{g} and hypermultiplets transforming in the representation \mathbf{R} of \mathfrak{g} , each chamber of $\text{I}(\mathfrak{g}, \mathbf{R})$ corresponds to a unique Coulomb phase of the Coulomb of the theory. Such a gauge theory can be obtained by a compactification of M-theory on an elliptic fibration with associated Lie algebra \mathfrak{g} and representation \mathbf{R} .

The fibral divisors D_i of the elliptic fibration correspond to the roots α_i of \mathfrak{g} . In codimension-two, the generic curve C_i of D_i can degenerate into a collection of rational curves. Each of these rational curves has intersections defining a weight ϖ , which will be an extremal weight of $\text{I}(\mathfrak{g}, \mathbf{R})$. Each crepant resolution of the underlying Weierstrass model, Y , corresponds to a relative minimal model over Y . Each of these relative minimal models corresponds to a unique chamber of the hyperplane arrangement $\text{I}(\mathfrak{g}, \mathbf{R})$. The extremal weights depend on the minimal model.

Definition 3.1. Given a curve C , its associated weight with respect to the fibral divisor D_i is the intersection number $-D_i \cdot C$. To any curve C , we can associate a weight vector $\varpi(C)$ with components $\varpi(C)_i = -D_i \cdot C$.

Remark 3.2. The decomposition of the curve C_i corresponding root α_i in a chamber Π with face ϖ_m^\perp are deduced using the linear relations connecting the extremal weights ϖ_m .

Remark 3.3. The intersection with D_0 can be deduced by linearity, using $D_0 \cong -\sum(m_i D_i)$, where m_i are the Dynkin coefficients of the highest root of \mathfrak{g} and D_i is the fibral divisor corresponding to the root α_i . If a curve C has negative intersection number with D_0 , this implies that C is contained in D_0 . In this case, C_0 will split with C being one of the components.

Figure 3, showed the Hasse diagram of the representation **56**, with a clear identification of the simple root between any two adjacent weights. We summarize the relevant data for the extremal weights here:

ϖ_{19}	$(1, 1, 1, \frac{1}{2}, 0, -\frac{1}{2}, \frac{1}{2})$	1 0 0 0 0 -1 0	(3.1)
$\varpi_{20} = \varpi_{19} - \alpha_1$	$(0, 1, 1, \frac{1}{2}, 0, -\frac{1}{2}, \frac{1}{2})$	-1 1 0 0 0 -1 0	
$\varpi_{23} = \varpi_{19} - \alpha_1 - \alpha_2$	$(0, 0, 1, \frac{1}{2}, 0, -\frac{1}{2}, \frac{1}{2})$	0 -1 1 0 0 -1 0	
$\varpi_{26} = \varpi_{19} - \alpha_1 - \alpha_2 - \alpha_3$	$(0, 0, 0, \frac{1}{2}, 0, -\frac{1}{2}, \frac{1}{2})$	0 0 -1 1 0 -1 1	
$\varpi_{29} = \varpi_{19} - \alpha_1 - \alpha_2 - \alpha_3 - \alpha_4$	$(0, 0, 0, -\frac{1}{2}, 0, -\frac{1}{2}, \frac{1}{2})$	0 0 0 -1 1 -1 1	
$\varpi_{32} = \varpi_{19} - \alpha_1 - \alpha_2 - \alpha_3 - \alpha_4 - \alpha_5$	$(0, 0, 0, -\frac{1}{2}, -1, -\frac{1}{2}, \frac{1}{2})$	0 0 0 0 -1 0 1	
$\varpi_{30} = \varpi_{19} - \alpha_1 - \alpha_2 - \alpha_3 - \alpha_7$	$(0, 0, 0, \frac{1}{2}, 0, -\frac{1}{2}, -\frac{1}{2})$	0 0 0 1 0 -1 -1	

including their expressions in both the basis of simple roots and the basis of fundamental weights. These two bases are used for different purposes in the analysis of the chambers.

Chambers	Conditions	Splitting curves	Weights
Ch ₁	$\phi_1 - \phi_6 < 0$	$C_0 \rightarrow C'_0 + C_{06}$ $C_6 \rightarrow 2C_{06} + 2C_1 + 2C_2 + 2C_3 + C_4 + C_7$	$C'_0 \rightarrow -\varpi_{19}$ $C_{06} \rightarrow -\varpi_{19}$
Ch ₂	$\phi_1 - \phi_6 > 0$ $-\phi_1 + \phi_2 - \phi_6 < 0$	$C_1 \rightarrow C'_1 + C_{16}$ $C_6 \rightarrow 2C_{16} + 2C_2 + 2C_3 + C_4 + C_7$	$C'_1 \rightarrow \varpi_{19}$ $C_{16} \rightarrow -\varpi_{20}$
Ch ₃	$-\phi_1 + \phi_2 - \phi_6 > 0$ $-\phi_2 + \phi_3 - \phi_6 < 0$	$C_2 \rightarrow C'_2 + C_{26}$ $C_6 \rightarrow 2C_{26} + 2C_3 + C_4 + C_7$	$C'_2 \rightarrow \varpi_{20}$ $C_{26} \rightarrow -\varpi_{23}$
Ch ₄	$-\phi_2 + \phi_3 - \phi_6 > 0$ $-\phi_3 + \phi_4 - \phi_6 + \phi_7 < 0$	$C_3 \rightarrow C'_3 + C_{36}$ $C_6 \rightarrow 2C_{36} + C_4 + C_7$	$C'_3 \rightarrow \varpi_{23}$ $C_{36} \rightarrow -\varpi_{26}$
Ch ₅	$-\phi_3 + \phi_4 - \phi_6 + \phi_7 > 0$ $\phi_4 - \phi_6 - \phi_7 < 0$ $-\phi_4 + \phi_5 - \phi_6 + \phi_7 < 0$	$C_4 \rightarrow C_{46} + C_{47}$ $C_6 \rightarrow C_{46} + C_{67}$ $C_7 \rightarrow C_{47} + C_{67}$	$C_{47} \rightarrow \varpi_{26}$ $C_{67} \rightarrow -\varpi_{30}$ $C_{46} \rightarrow -\varpi_{29}$
Ch ₆	$-\phi_4 + \phi_5 - \phi_6 + \phi_7 > 0$ $-\phi_5 + \phi_7 < 0$	$C_5 \rightarrow C'_5 + C_{57}$ $C_7 \rightarrow C_4 + C_6 + 2C_{57}$	$C_{57} \rightarrow \varpi_{29}$ $C'_5 \rightarrow -\varpi_{32}$
Ch ₇	$-\phi_4 + \phi_5 - \phi_6 + \phi_7 > 0$ $-\phi_5 + \phi_7 > 0$	$C_7 \rightarrow 2C'_7 + C_4 + 2C_5 + C_6$	$C'_7 \rightarrow -\varpi_{32}$
Ch ₈	$\phi_4 - \phi_6 - \phi_7 > 0$	$C_4 \rightarrow 2C'_4 + C_6 + C_7$	$C'_4 \rightarrow \varpi_{30}$

Table 1: Chambers and fiber degenerations of an E_7 -model. The chambers are defined with respect to the interior walls ϖ_m^\perp for $m = 19, 20, 23, 26, 29, 30$. These inequalities are imposed on the interior of the dual fundamental Weyl chamber $\langle \alpha_i, \phi \rangle > 0$ $i = 1, 2, 3, 4, 5, 6, 7$. All the weights appearing in the right column are weights of the representation **56**. In chambers Ch₄, Ch₅, Ch₆, and Ch₈, the weights are also obtained geometrically by studying the splitting of curves after a resolution of singularities [25].

Our algorithm for determining the fiber degeneration in each chamber consists of the following steps:

- Identifying extremal weights by noting the interior walls of each chamber. This will be some subset of the weights appearing in the sign vector $(\varpi_m$ for $m \in \{19, 20, 23, 26, 29, 30\}$), which can be read off of Figure 4.
- Expressing these extremal weights in the basis of simple roots (see equation (3.1)) to identify the degeneration of the components of the generic fiber into rational effective curves.
- Expressing extremal weights in the basis of fundamental weights (see equation (3.1)) to get the intersection numbers of the corresponding curve with the fibral divisors. As explained in Remark 3.3, intersection with D_0 can be computed using linearity. Explicitly, for any curve C , we have

$$D_0 \cdot C = -(2D_1 + 3D_2 + 4D_3 + 3D_4 + 2D_5 + D_6 + 2D_7) \cdot C. \quad (3.2)$$

The above method is applied to each chamber in Appendix A and our results are summarized in Table 1 and illustrated in Figure 6. We confirm the analysis of [12] and correct few inaccuracies in [27] such as the splitting rules for the curve C_6 in Chamber 1.

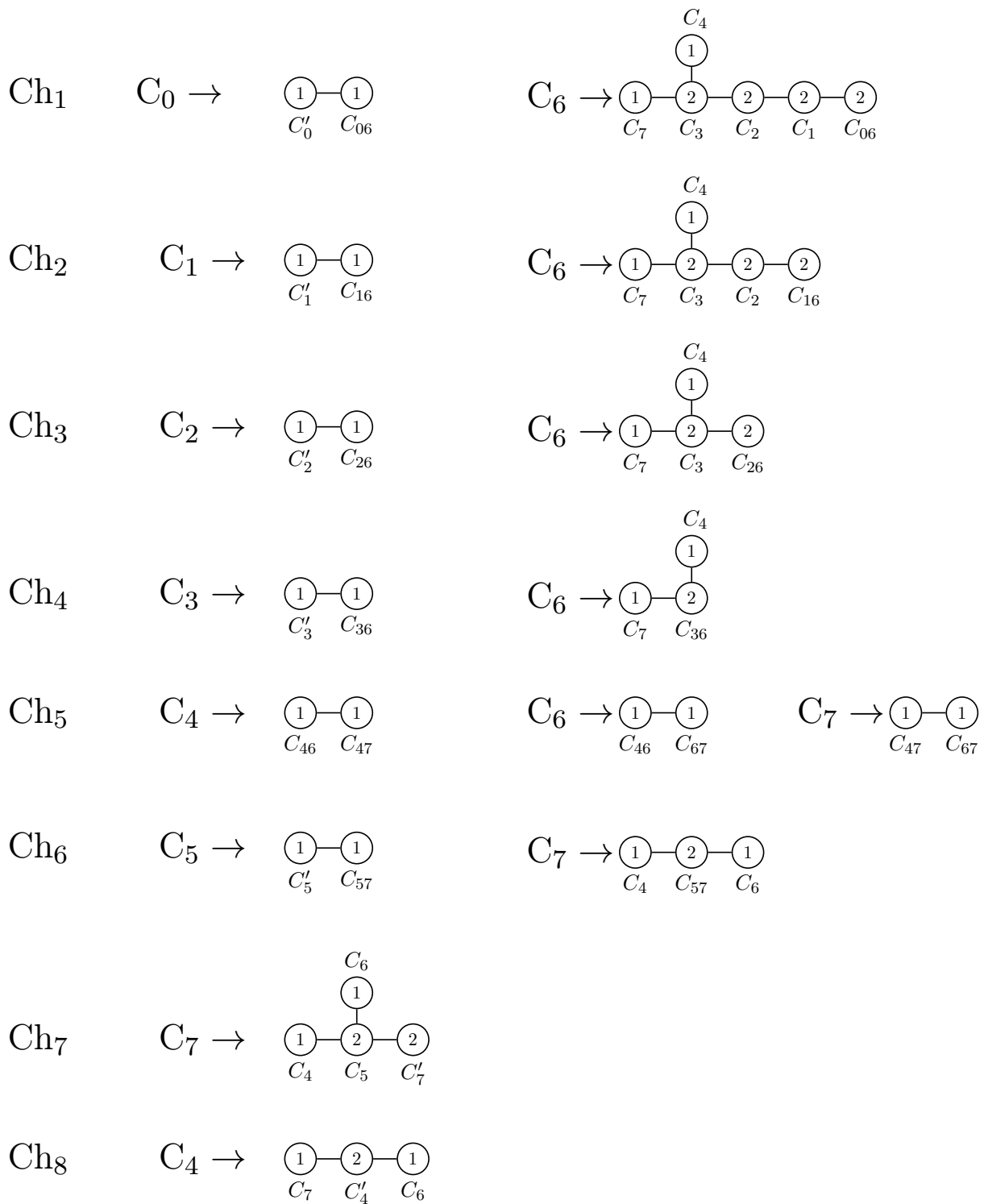


Figure 6: In each chamber, the decomposition of the III* fiber is only possible if some of the nodes degenerate. We give the decomposition for all fibers over $V(s, a)$. For more information, see Appendix A.

Ch ₁	Ch ₂	Ch ₃	Ch ₄	Ch ₅	Ch ₆	Ch ₇	Ch ₈
VIII	VII	VI	V	IV	II	III	I

Table 2: Dictionary between our conventions and those of reference [12].

In [12, Section 4], Diaconescu and Entin identified the Coulomb chambers of an E_7 -gauge theory with matter transforming in the representation **56**.⁵ The dictionary between our conventions (Ch_i) for the chambers of $I(E_7, \mathbf{56})$ and those of [12] (I–VIII) is given in Table 2.

Reference [12] also gave the degeneration of the components of the fiber III*, however, the description of chamber Ch_1 was incomplete as the splitting of the affine node was not specified. For Chamber 1 we find (see Appendix A for details)

$$\text{Degeneration in Chamber 1: } \begin{cases} C_0 \rightarrow C'_0 + C_{06}, \\ C_6 \rightarrow 2C_{06} + 2C_1 + 2C_2 + 2C_3 + C_4 + C_7. \end{cases} \quad (3.3)$$

Our results can be compared with other findings in the literature. In [27], the chambers of an E_7 -model with matter in the representation **56** were re-analyzed. In particular, the splitting for the affine node in Chamber 1 was explicitly discussed. Unfortunately, the description of Chamber 1 in [27] has two important inaccuracies (see Section A.1): the splitting of the fiber C_6 is incorrect as written as it misses the component C_4 , and the weight of the node of appearing in the degeneration of C_0 is also inaccurate. The curve representing the zero node has weights $[0, 0, 0, 0, 0, 1, 0]$ in the basis of fundamental weights and therefore corresponds to the highest weight of the representation **56**. In the notation of [27], that should be L_7 and not the weight (7).

Reference [11] examined the geometry of E_7 -models for which the divisor S supporting the fiber of type III* is assumed to be a smooth rational curve of self-intersection -8 or -7 . For a (-8) -curve, the authors of [11] conclude that the fibral divisors are Hirzebruch surfaces that intersect transversally. In particular, the fiber III* does not degenerate to a more singular fiber. However when the curve S is of self-intersection -7 , there are necessarily singular fibers that carry the weights of the representation **56**. In our notation, the claim of [11] is that only one fibral divisor is not Hirzebruch and this divisor is D_0 or D_6 and that only one new extremal curve appears in the degeneration. However, the analysis of [11] does not agree with any of the chambers of an E_7 -model with matter in the representation **56** and is in contradiction with both [12] and [27].

⁵See the inequalities listed in equations (4.6), (4.10), (4.11), (4.16), (4.19), and (4.21) of [12, Section 4], which are reproduced here in Table 1.

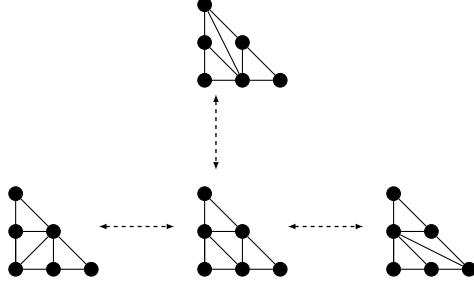


Figure 7: Flops between the four crepant resolutions of the singularity $\mathbb{C}[u_1, u_2, u_3, t]/(t^2 - u_1u_2u_3)$.

This provides a direct proof of the D_4 flop structure between the chambers examined in [25]. There we considered a different set of blowups to resolve the four shaded chambers in Figure 4. To understand the flops between $Y_4, Y_5,$ and $Y_8,$ we considered

$$\begin{array}{ccccccccccc}
 X_0 & \xleftarrow{(x, y, s|e_1)} & X_1 & \xleftarrow{(x, y, e_1|e_2)} & X_2 & \xleftarrow{(y, e_1, e_2|e_3)} & X_3 & \xleftarrow{(y, e_2|e_4)} & X_4 & \xleftarrow{(e_2, e_4|e_5)} & X_5 & \xleftarrow{(y, e_3|e_6)} & X_6 & \xleftarrow{(e_3, e_6|e_7)} & X_7^+ \\
 & & & & & & & & & & & & & \xleftarrow{(e_3, e_4|e_7)} & X_7^- \\
 & & & & & & & & & & & & & \xleftarrow{(y, e_3|e_7)} & X_7' \\
 & & & & & & & & & & & & & \xleftarrow{(e_3, e_4|e_6)} & X_6'
 \end{array} \tag{4.5}$$

where $Y_4, Y_5,$ and Y_8 are the proper transforms of $X_7^+, X_7^-,$ and $X_7',$ respectively. To understand the flops between $Y_4, Y_5,$ and $Y_6,$ we considered

$$\begin{array}{ccccccccccc}
 X_0 & \xleftarrow{(x, y, s|e_1)} & X_1 & \xleftarrow{(y, e_1|e_2)} & X_2 & \xleftarrow{(x, y, e_2|e_3)} & X_3 & \xleftarrow{(x, e_2, e_3|e_4)} & X_4 & \xleftarrow{(e_2, e_4|e_5)} & X_5 & \xleftarrow{(e_2, e_5|e_6)} & X_6^+ \\
 & & & & & & & & & & & & \xleftarrow{(e_2, e_3|e_6)} & X_6^- \\
 & & & & & & & & & & & & \xleftarrow{(e_2, e_4|e_6)} & X_6'
 \end{array} \tag{4.6}$$

where $Y_4, Y_5,$ and Y_6 are the proper transforms of $X_6^+, X_6^-,$ and $X_6',$ respectively. In addition to allowing an explicit proof of the D_4 -flops of the E_7 -model, the new sequence of blowups (4.1) will simplify our triple intersection computations in Section 5.⁶

⁶ While blowups (4.6) and (4.6) were sufficient to resolve the respective varieties and study the flop structure in [25], if one were to continue to use them to compute triple intersection numbers via the techniques laid out in Section 5, one would need to append the following additional blowups

$$X_7^+ \xleftarrow{(e_1, e_6|e_8)} X_8^+, \quad X_7^- \xleftarrow{(y, e_1|e_8)} X_8^-, \quad X_6' \xleftarrow{(x, e_2|e_7)} X_7'', \quad X_7' \xleftarrow{(y, e_1|e_8)} X_8' \tag{4.7}$$

to compute triple intersections in $Ch_4, Ch_5, Ch_6,$ and $Ch_8,$ respectively. This is safe to do since blowing-up a variety along a smooth locus is an isomorphism. Such additional blowups can be interpreted as auxiliary blowups requested by excess intersections. Upon doing so we can use the exceptional divisor as a clean Cartier divisor.

5 Triple intersection numbers

We begin with some pushforward theorems needed to perform our triple intersection computations.

Definition 5.1 (Resolution of singularities). A resolution of singularities of a variety Y is a proper birational morphism $\varphi : \tilde{Y} \rightarrow Y$ such that \tilde{Y} is nonsingular and φ is an isomorphism away from the singular locus of Y .

Definition 5.2 (Crepanant birational map). A birational map $\varphi : \tilde{Y} \rightarrow Y$ between two algebraic varieties with \mathbb{Q} -Cartier canonical classes is said to be *crepanant* if it preserves the canonical class.

Theorem 5.3 (Aluffi, [1, Lemma 1.3]). *Let $Z \subset X$ be the complete intersection of d nonsingular hypersurfaces Z_1, \dots, Z_d meeting transversally in X . Let $f : \tilde{X} \rightarrow X$ be the blowup of X centered at Z . We denote the exceptional divisor of f by E . The total Chern class of \tilde{X} is then:*

$$c(T\tilde{X}) = (1 + E) \left(\prod_{i=1}^d \frac{1 + f^*Z_i - E}{1 + f^*Z_i} \right) f^*c(TX).$$

Theorem 5.4 (Esole–Jefferson–Kang, see [18]). *Let the nonsingular variety $Z \subset X$ be a complete intersection of d nonsingular hypersurfaces Z_1, \dots, Z_d meeting transversally in X . Let E be the class of the exceptional divisor of the blowup $f : \tilde{X} \rightarrow X$ centered at Z . Let $\tilde{Q}(t) = \sum_a f^*Q_a t^a$ be a formal power series with $Q_a \in A_*(X)$. We define the associated formal power series $Q(t) = \sum_a Q_a t^a$, whose coefficients pullback to the coefficients of $\tilde{Q}(t)$. Then the pushforward $f_*\tilde{Q}(E)$ is*

$$f_*\tilde{Q}(E) = \sum_{\ell=1}^d Q(Z_\ell)M_\ell, \quad \text{where} \quad M_\ell = \prod_{\substack{m=1 \\ m \neq \ell}}^d \frac{Z_m}{Z_m - Z_\ell}.$$

Theorem 5.5 (See [18] and [2, 3, 24, 26]). *Let \mathcal{L} be a line bundle over a variety B and $\pi : X_0 = \mathbb{P}[\mathcal{O}_B \oplus \mathcal{L}^{\otimes 2} \oplus \mathcal{L}^{\otimes 3}] \rightarrow B$ a projective bundle over B . Let $\tilde{Q}(t) = \sum_a \pi^*Q_a t^a$ be a formal power series in t such that $Q_a \in A_*(B)$. Define the auxiliary power series $Q(t) = \sum_a Q_a t^a$. Then*

$$\pi_*\tilde{Q}(H) = -2 \left. \frac{Q(H)}{H^2} \right|_{H=-2L} + 3 \left. \frac{Q(H)}{H^2} \right|_{H=-3L} + \frac{Q(0)}{6L^2},$$

where $L = c_1(\mathcal{L})$ and $H = c_1(\mathcal{O}_{X_0}(1))$ is the first Chern class of the dual of the tautological line bundle of $\pi : X_0 = \mathbb{P}(\mathcal{O}_B \oplus \mathcal{L}^{\otimes 2} \oplus \mathcal{L}^{\otimes 3}) \rightarrow B$.

The above theorems are enough for most applications of intersection theory to elliptic fibrations. Since our blowups involve regular sequences (c.f. Fulton) of length two or three, we can use:

Theorem 5.6 (See [18, Lemma 3.4]). *For a blowup f with center (Z_1, Z_2) , exceptional divisor E*

$$f_*E = 0, \quad f_*E^2 = -Z_1Z_2, \quad f_*E^3 = -(Z_1 + Z_2)Z_1Z_2, \quad f_*E^4 = -(Z_1^2 + Z_2^2 + Z_1Z_2)Z_1Z_2.$$

For a blowup f with the complete intersection (Z_1, Z_2, Z_3) as its center and exceptional divisor E

$$f_*E = 0, \quad f_*E^2 = 0, \quad f_*E^3 = Z_1Z_2Z_3, \quad f_*E^4 = (Z_1 + Z_2)Z_1Z_2Z_3.$$

We are now ready to compute the triple intersection numbers of the fibral divisors for the cases for which an explicit crepant resolution is available. The triple intersection polynomial is by definition

$$F = \int \left(\sum_{a=0}^7 D_a \phi_a \right)^3 [Y] = \int_B \pi_* f_{1*} f_{2*} f_{3*} f_{4*} f_{5*} f_{6*} f_{7*} f_{8*} \left[\left(\sum_{a=0}^7 D_a \phi_a \right)^3 [Y] \right], \quad (5.1)$$

where f_i is the i -th blowup and $\pi : X_0 = \mathbb{P}[\mathcal{O}_B \oplus \mathcal{L}^{\otimes 2} \oplus \mathcal{L}^{\otimes 3}] \rightarrow B$ is the map defining the projective bundle. Using the pushforward theorems discussed above, the triple intersection polynomial can be expressed in terms of intersection numbers in the base B .

The intersection polynomials are computed in Appendix B below. We consider the tree of blowups (4.1) and each of the triple intersections is computed by successively applying Theorem 5.6 or Theorem 5.4 to pushforward the intersection computation to X_0 and finally using Theorem 5.5 to pushforward to the base.⁷

In the Calabi–Yau threefold case, we have

$$L = -K, \quad S \cdot L = 2 - 2g + S^2. \quad (5.2)$$

The matter representations are the adjoint and the **56**. The number of hypermultiplets charged under these are functions of the genus and self-intersection number of S :

$$n_A = g, \quad n_F = \frac{1}{2} V(a) \cdot S = 4(1 - g) + \frac{1}{2} S^2. \quad (5.3)$$

The non-negativity of n_A and n_F implies a bound on the self-intersection of S :

$$S^2 \geq -8(1 - g). \quad (5.4)$$

Remark 5.7. There are no adjoint hypermultiplets when $g = 0$ and no matter in the representation **56** when $n_F = 0$, which means $S^2 = -8(1 - g)$. In particular, when $g = 0$ and $S^2 = -8$, we find that all four of the triple intersection polynomials (see Theorem 5.9) reduce to

$$\begin{aligned} F(\phi) = & 8(\phi_0^3 + \phi_1^3 + \phi_2^3 + \phi_3^3 + \phi_4^3 + \phi_5^3 + \phi_6^3 + \phi_7^3) - 6(-2\phi_0^2\phi_1 + 3\phi_0\phi_1^2) \\ & - 6(\phi_1^2\phi_2 + \phi_2^2\phi_3 + \phi_3^2\phi_4 + \phi_4^2\phi_5 - \phi_4\phi_5^2 + 2\phi_1\phi_2^2 + 2\phi_4^2\phi_5 - 2\phi_5\phi_6^2 + 3\phi_5^2\phi_6) \end{aligned} \quad (5.5)$$

Remark 5.8 (Odd self-intersection and half-hypermultiplets). When S^2 is odd, n_F is a half-integer. This is possible since the representation **56** is pseudo-real and thus allows half-hypermultiplets. In particular, if $g = 0$ and $S^2 = -7$, we have one half-hypermultiplet at $V(a) \cap S$ since $n_F = \frac{1}{2}$.

⁷The only challenge arises when it is not obvious how to express the fibral divisor as a neat Cartier divisor. In some cases, when it is only defined as a complete intersection $g_1 = g_2 = 0$, we can use an excess intersection formula. Equivalently, one can just perform another blowup with center (g_1, g_2) (see footnote 6).

Theorem 5.9. *For a Calabi–Yau threefold Y defined as the crepant resolution of an E_7 Weierstrass model and corresponding to the chamber i ($i = 4, 5, 6, 8$), the cubic intersection polynomials reduce to $F_i(\phi)$ and are as follows:*

$$\begin{aligned}
F_4(\phi) = & 8(1-g)(\phi_0^3 + \phi_1^3 + \phi_2^3 + \phi_4^3 + \phi_5^3 + \phi_7^3) - S^2\phi_3^3 - 2(4-4g+S^2)\phi_6^3 \\
& - 3(4-4g+S^2)\phi_0^2\phi_1 + 3(2-2g+S^2)\phi_0\phi_1^2 + 3(6-6g+S^2)\phi_1^2\phi_2 + 3(4-4g+S^2)\phi_1\phi_2^2 \\
& - 3(8-8g+S^2)(\phi_3\phi_2^2 + \phi_3^2\phi_6 + \phi_3\phi_6^2 + 2\phi_4^2\phi_6 + 2\phi_6\phi_7^2) \\
& + 3(6-6g+S^2)\phi_3^2\phi_2 - 6(11-11g+S^2)\phi_5^2\phi_6 + 6(10-10g+S^2)\phi_5\phi_6^2 \\
& + 6(-1+g)(\phi_3^2\phi_4 + \phi_3^2\phi_7 + 2\phi_4^2\phi_5 - \phi_4\phi_5^2) \\
& + 6(8-8g+S^2)(\phi_3\phi_4\phi_6 + \phi_4\phi_5\phi_6 + \phi_3\phi_6\phi_7)
\end{aligned} \tag{5.6}$$

$$\begin{aligned}
F_5(\phi) = & 8(1-g)(\phi_0^3 + \phi_1^3 + \phi_2^3 + \phi_3^3 + \phi_5^3) - S^2(\phi_4^3 + \phi_6^3 + \phi_7^3) \\
& - 3(8-8g+S^2)(\phi_3\phi_2^2 - \phi_3\phi_4^2 + \phi_4\phi_6^2 + \phi_4\phi_7^2 + \phi_6\phi_7^2 + \phi_4^2\phi_6 + \phi_6^2\phi_7 - \phi_3\phi_7^2 + \phi_7\phi_4^2) \\
& - 3(4-4g+S^2)\phi_1\phi_0^2 + 3(2-2g+S^2)\phi_1^2\phi_0 + 3(6-6g+S^2)\phi_2\phi_3^2 - \phi_1^2\phi_2) \\
& + 3(10-10g+S^2)(2\phi_5\phi_6^2 - \phi_3^2\phi_4 - \phi_3^2\phi_7) + 3(4-4g+S^2)\phi_1\phi_2^2 - 6(11-11g+S^2)\phi_5^2\phi_6 \\
& + 6(-1+g)(2\phi_4^2\phi_5 - \phi_4\phi_5^2) + 6(8-8g+S^2)(\phi_4\phi_5\phi_6 + \phi_3\phi_4\phi_7 + \phi_4\phi_6\phi_7)
\end{aligned} \tag{5.7}$$

$$\begin{aligned}
F_6(\phi) = & 8(1-g)(\phi_0^3 + \phi_1^3 + \phi_2^3 + \phi_3^3 + \phi_4^3 + \phi_6^3) - S^2\phi_5^3 - 2(4-4g+S^2)\phi_7^3 \\
& + 6(8-8g+S^2)(\phi_3\phi_4\phi_7 + \phi_4\phi_5\phi_7 + \phi_5\phi_6\phi_7) + 3(2-2g+S^2)\phi_0\phi_1^2 \\
& - 3(8-8g+S^2)(\phi_3\phi_2^2 - \phi_3\phi_4^2 - \phi_3\phi_7^2 + \phi_5\phi_7^2 + 2\phi_4^2\phi_7 + \phi_5^2\phi_7 + 2\phi_6^2\phi_7) \\
& - 3(4-4g+S^2)(\phi_1\phi_0^2 - \phi_1\phi_2^2) + 3(6-6g+S^2)(\phi_2\phi_3^2 - \phi_1^2\phi_2) - 3(14-14g+S^2)\phi_5^2\phi_6 \\
& + 3(10-10g+S^2)(\phi_4\phi_5^2 - \phi_3^2\phi_7 - \phi_3^2\phi_4) + 3(12-12g+S^2)(\phi_5\phi_6^2 - \phi_4^2\phi_5)
\end{aligned} \tag{5.8}$$

$$\begin{aligned}
F_8(\phi) = & 8(1-g)(\phi_0^3 + \phi_1^3 + \phi_2^3 + \phi_3^3 + \phi_5^3 + \phi_6^3 + \phi_7^3) - 2(4-4g+S^2)\phi_4^3 \\
& + 3(2-2g+S^2)\phi_0\phi_1^2 - 3(4-4g+S^2)\phi_0^2\phi_1 \\
& + 3(4-4g+S^2)\phi_1\phi_2^2 - 3(6-6g+S^2)\phi_1^2\phi_2 + 3(6-6g+S^2)\phi_2\phi_3^2 - 3(8-8g+S^2)\phi_2^2\phi_3 \\
& + 6(10-10g+S^2)\phi_5\phi_6^2 - 6(11-11g+S^2)\phi_5^2\phi_6 - 3(10-10g+S^2)\phi_3^2\phi_7 \\
& + 6(1-g)\phi_4\phi_5^2 - 3(10-10g+S^2)\phi_3^2\phi_4 + 12(-1+g)\phi_4^2\phi_5 \\
& - 6(8-8g+S^2)\phi_4(\phi_6^2 - \phi_5\phi_6 + \phi_7^2) + 3(8-8g+S^2)\phi_3(\phi_4 + \phi_7)^2.
\end{aligned} \tag{5.9}$$

6 Isomorphism classes of fibral divisors

In this section, we determine the isomorphism classes of the fibral divisors that are projective bundles in the relative minimal models Y_4, Y_5, Y_6 , and Y_8 , using their known crepant resolutions. The results are listed in Table 3.

When the fiber C_a does not degenerate, the fibral divisor D_a ($a = 0, 1, \dots, 7$) is a ruled surface $D_a \rightarrow S$ isomorphic to a \mathbb{P}^1 -bundle over the divisor S supporting the E_7 fiber. Since we only have two line bundles available, namely \mathcal{L} and \mathcal{S} , we expect to have projective bundles of the form⁸

$$\mathbb{P}_S(\mathcal{S}^{\otimes p} \oplus \mathcal{L}^{\otimes q}),$$

where p and q are integer numbers. There are two methods of finding p and q . The first method is akin to that used in [17], where one keeps track of the rescaling freedom after each blowup in order to identify the class of the relative projective coordinates. The second method uses intersection theory results from the previous section. We will take the intersection theoretic approach here and include an example scaling computation in Appendix C.

	Y_4	Y_5	Y_6	Y_8
D_0	$\mathbb{P}_S(\mathcal{O}_S \oplus \mathcal{L})$	$\mathbb{P}_S(\mathcal{O}_S \oplus \mathcal{L})$	$\mathbb{P}_S(\mathcal{O}_S \oplus \mathcal{L})$	$\mathbb{P}_S(\mathcal{O}_S \oplus \mathcal{L})$
D_1	$\mathbb{P}_S(\mathcal{S} \oplus \mathcal{L}^{\otimes 2})$	$\mathbb{P}_S(\mathcal{S} \oplus \mathcal{L}^{\otimes 2})$	$\mathbb{P}_S(\mathcal{S} \oplus \mathcal{L}^{\otimes 2})$	$\mathbb{P}_S(\mathcal{S} \oplus \mathcal{L}^{\otimes 2})$
D_2	$\mathbb{P}_S(\mathcal{S}^{\otimes 2} \oplus \mathcal{L}^{\otimes 3})$	$\mathbb{P}_S(\mathcal{S}^{\otimes 2} \oplus \mathcal{L}^{\otimes 3})$	$\mathbb{P}_S(\mathcal{S}^{\otimes 2} \oplus \mathcal{L}^{\otimes 3})$	$\mathbb{P}_S(\mathcal{S}^{\otimes 2} \oplus \mathcal{L}^{\otimes 3})$
D_3	N/A	$\mathbb{P}_S(\mathcal{S}^{\otimes 3} \oplus \mathcal{L}^{\otimes 4})$	$\mathbb{P}_S(\mathcal{S}^{\otimes 3} \oplus \mathcal{L}^{\otimes 4})$	$\mathbb{P}_S(\mathcal{S}^{\otimes 3} \oplus \mathcal{L}^{\otimes 4})$
D_4	$\mathbb{P}_S(\mathcal{S} \oplus \mathcal{L})$	N/A	$\mathbb{P}_S(\mathcal{S}^{\otimes 4} \oplus \mathcal{L}^{\otimes 5})$	N/A
D_5	$\mathbb{P}_S(\mathcal{S}^{\otimes 2} \oplus \mathcal{L}^{\otimes 2})$	$\mathbb{P}_S(\mathcal{S}^{\otimes 2} \oplus \mathcal{L}^{\otimes 2})$	N/A	$\mathbb{P}_S(\mathcal{S}^{\otimes 2} \oplus \mathcal{L}^{\otimes 2})$
D_6	N/A	N/A	$\mathbb{P}_S(\mathcal{S}^{\otimes 6} \oplus \mathcal{L}^{\otimes 7})$	$\mathbb{P}_S(\mathcal{S}^{\otimes 9} \oplus \mathcal{L}^{\otimes 11})$
D_7	$\mathbb{P}_S(\mathcal{S} \oplus \mathcal{L})$	N/A	N/A	$\mathbb{P}_S(\mathcal{S}^{\otimes 4} \oplus \mathcal{L}^{\otimes 5})$

Table 3: Fibral divisors that are projective bundles. We write N/A when a divisor is not a projective bundle. If the base is of dimension three or higher, D_6 is not a projective bundle unless $V(a, b) \cap S$ is empty. Otherwise it contains a full rational surface over the locus $V(a, b) \cap S$. We examine this possibility in Section 8.

We will now describe the steps to derive Table 3. Let X be a \mathbb{P}^1 -bundle over a smooth variety S of the type

$$\pi : X = \mathbb{P}_S(\mathcal{O}_S \oplus \mathcal{D}) \rightarrow S, \quad (6.1)$$

where \mathcal{D} is a line bundle over S . Let $[u_0 : u_1]$ be projective coordinates along the fiber of X with u_0 a section of $\mathcal{O}_X(1)$ and u_1 a section of $\mathcal{O}_X(1) \otimes \pi^*\mathcal{D}$. Let J denote the first Chern class of the line bundle $\mathcal{O}_X(1)$, and D denote the first Chern class of \mathcal{D} . The divisors $V(u_0)$ and $V(u_1)$ define sections of π corresponding to the classes J and $J + \pi^*D$ in the Chow ring.

The total Chern class of X is

$$c(TX) = (1 + J)(1 + J + \pi^*D)\pi^*c(TS). \quad (6.2)$$

⁸As in Section 2.1, we use the symbol \mathcal{S} to denote the line bundle for which the divisor S is the zero locus of a smooth section.

In particular, we have

$$c_1(TX) = 2J + \pi^*D + \pi^*c_1(TS). \quad (6.3)$$

We can compute the pushforwards π_*J^k using the functorial properties of the Segre map. The key formula is:

$$\pi_*\frac{1}{1-J} \cap [X] = \frac{1}{1+D} \cap [S], \quad (6.4)$$

or equivalently

$$\pi_*([X] + J \cap [X] + J^2 \cap [X] + \dots) = [S] - D \cap [S] + D^2 \cap [S] - D^3 \cap [S] + \dots. \quad (6.5)$$

By matching terms of the same dimensionality, we get:

$$\pi_*1 = 0, \quad \pi_*J = 1, \quad \pi_*J^2 = -D, \quad \pi_*J^{k+1} = (-1)^k D^k \quad (k > 1). \quad (6.6)$$

We now assume that S is a smooth curve of genus g . Then, X is a geometrically ruled surface. Before proceeding further, let us recall some facts about ruled surfaces.

Definition 6.1. A *smooth compact projective curve* is a curve isomorphic to the projective line \mathbb{P}^1 . A *ruled surface* is a morphism $\pi : X \rightarrow S$ such that the generic fiber is a smooth compact rational curve. A smooth morphism $\pi : X \rightarrow S$ is called a *geometric ruled surface* if all its fibers are isomorphic to a smooth projective rational curve.

Let S be a curve of genus g . If we denote the class of a fiber by f , then there is an irreducible curve of class h_- and self-intersection $-n$ ($n \geq 0$) defining a section such that the canonical class of X satisfies

$$-K_X = 2h_- + (n + 2 - 2g)f. \quad (6.7)$$

There is also an irreducible curve of class $h_+ = h_- + nf$ with self-intersection n . The curves of class h_{\pm} both define sections of X and they don't intersect

$$f^2 = 1, \quad h_{\pm}^2 = \pm n, \quad h_+ \cdot h_- = 0, \quad h_{\pm} \cdot f = 1. \quad (6.8)$$

The integer n is called the invariant of the ruled surface.

We now apply this to the fibral divisor X defined in equation (6.1). Since a projective bundle is a flat fibration, all fibers have the same class f . At the level of the Chow group, the generators of $A(X)$ are J and f . The degree of D in S is n and we have:

$$\int_X J \cdot \pi^*D = \int_S \pi_*J \cdot D = \int_S D = \int_S D \cdot S = n, \quad [\pi^*D] = n[f], \quad (6.9)$$

so that

$$\int_X f \cdot J = \int_{\mathbb{P}^1} c_1(\mathcal{O}_{\mathbb{P}^1}(1)) = 1, \quad \int_X f^2 = \int_{\mathbb{P}^1} c_1(\mathcal{O}_{\mathbb{P}^1}) = 0. \quad (6.10)$$

$$\int_X J^2 = -n, \quad \int_X J \cdot (J + \pi^*D) = 0, \quad \int_X (J + \pi^*D)^2 = n. \quad (6.11)$$

We are now ready to derive Table 3. For a fibral divisor which is a \mathbb{P}^1 -projective bundle, we can

determine its type by identifying two non-trivial classes r_1 and r_2 which correspond to two irreducible curves, as well as a line bundle \mathcal{D} over S with first Chern class D such that $r_1^2 + r_2^2 = r_1 r_2 = 0$ and $\int_X r_1^2 = DS$. In that situation, we deduce that $X \cong \mathbb{P}_S(\mathcal{O}_S \oplus \mathcal{D})$:

$$\left\{ \begin{array}{l} r_1^2 + r_2^2 = 0 \\ r_1 r_2 = 0 \\ r_1^2 = DS \end{array} \right\} \implies X \cong \mathbb{P}_S(\mathcal{O}_S \oplus \mathcal{D}). \quad (6.12)$$

The results are listed in Table 4, which requires the pushforward formulas of Section 5 and divisor class computations in Appendix B. We deduce Table 3 directly from Table 4.

The following theorem explains how different projective bundles are related to each other.

Theorem 6.2. *Let $\rho : Y \rightarrow B$ be an elliptic fibration defined by a crepant resolution of a Weierstrass model over a base B . Let D_a and D_b be two divisors of Y such that $\rho_*(D_a D_b) = S$. Then*

$$\rho_*(D_a^2 D_b + D_a D_b^2) = (S - L)S. \quad (6.13)$$

Proof. If we denote by η_{ab} the intersection of two adjacent divisors D_a and D_b , then

$$K_{\eta_{ab}} = K_Y + D_a + D_b, \quad (6.14)$$

$$\chi(\eta_{ab}) = -K_{\eta_{ab}} D_a D_b = -(K_Y + D_a + D_b) D_a D_b. \quad (6.15)$$

But since η_{ab} is isomorphic to S , we also have

$$\chi(\eta_{ab}) = -(K_B + S)S. \quad (6.16)$$

Since $K_Y = K_B + L$ and $\eta_{ab} = D_a D_b$ pushes forward to S for any ADE model, we get

$$\rho_*(D_a^2 D_b + D_a D_b^2) = -(K_B + L)S - \chi(S) = -(K_B + L)S + (K_B + S)S = (S - L)S. \quad (6.17)$$

□

7 Characteristic numbers of fibral divisors

In this section, we give the linear functions induced on $H^2(Y, \mathbb{Z})$ for the second Chern class of the minimal models $Y = \{Y_4, Y_5, Y_6, Y_8\}$, as well as characteristic numbers of their fibral divisors. In particular, we consider the signature $\tau(D)$ and also the ordinary $\chi(D)$ and holomorphic $\chi_0(D)$ Euler characteristics. This data provides information about the structure of the fibral divisors. We assume that the minimal models are threefolds, thus, these characteristic numbers are all functions of the Chern numbers $c_1^2(D_a)$ and $c_2(D_a)$. Characteristic numbers for elliptic fibrations are computed in [19, 20].

	R_1	R_2	Y_4	Y_5	Y_6	Y_8
D_0	D_1	$\frac{1}{3}H$	LS	LS	LS	LS
D_1	D_0	D_2	$-(2L - S)S$	$-(2L - S)S$	$-(2L - S)S$	$-(2L - S)S$
D_2	D_1	D_3	$-(3L - 2S)S$	$-(3L - 2S)S$	$-(3L - 2S)S$	$-(3L - 2S)S$
D_3	D_2	D_4	N/A	$-(4L - 3S)S$	$-(4L - 3S)S$	$-(4L - 3S)S$
D_4	D_3	D_5	$-(L - S)S$	N/A	$-(5L - 4S)S$	N/A
D_5	D_4	x	$-(2L - 2S)S$	$-(2L - 2S)S$	N/A	$-(2L - 2S)S$
D_6	D_5	y	N/A	N/A	$-(7L - 6S)S$	$-(11L - 9S)S$
D_7	D_3	y	$-(L - S)S$	N/A	N/A	$-(5L - 4S)S$

Table 4: For each fibral divisor D_a , we present a divisor R_1 and a divisor R_2 such that the divisor R_1 defines, by intersection, a section of $D_a \rightarrow S$. The divisor R_2 is such that $D_a R_1^2 = -D_a R_2^2$ and $R_1 R_2 D_a = 0$. An N/A indicates when these conditions do not hold. When D_a is a \mathbb{P}^1 -bundle and has $D_a R_1^2 = \pm(pL - qS)S$, we deduce that D_a is isomorphic to $\mathbb{P}_S(\mathcal{S}^{\otimes q} \oplus \mathcal{L}^{\otimes p})$ as listed in Table 3.

Given a threefold Y , the second Chern class defines a linear form on $H^2(Y, \mathbb{Z})$

$$\mu : H^2(Y, \mathbb{Z}) \rightarrow \mathbb{Z} \quad D \mapsto \int_Y D \cdot c_2(TY).$$

Knowing the properties of this linear form is important for several reasons. For one, Wilson showed that the linear form μ plays a central role in the classification of Calabi–Yau varieties [39]. The second Chern class also appears in the Hirzebruch–Riemann–Roch theorem and is used in the computation of the microscopic entropy attached to a very ample divisor D in a Calabi–Yau threefold [34].

Theorem 7.1. *For each of the minimal models Y_4 , Y_5 , Y_6 , and Y_8 of an E_7 -model, the second Chern class induces the following linear action on the divisors*

$$\begin{aligned} c_2(TY) \cdot \varphi^* H &= 3 \left(c_2(TB) - c_1(TB)L \right), \\ c_2(TY) \cdot \varphi^* \pi^* \alpha &= 12L \cdot \alpha, \\ c_2(TY) \cdot D_a &= 2(L - S)S, \end{aligned}$$

where $H = c_1(\mathcal{O}_{X_0}(1))$, φ is the crepant resolution, π is the projection of the projective bundle X_0 over the base B , and α is a class of the Chow ring of the base. We note the following exceptions for each minimal model:

$$\begin{aligned} Y_4 : \quad c_2(TY) \cdot D_3 &= 2(3L - 2S)S, \quad c_2(TY) \cdot D_6 = 2(7L - 5S)S, \\ Y_5 : \quad c_2(TY) \cdot D_4 &= 2(3L - 2S)S, \quad c_2(TY) \cdot D_5 = 2(3L - 2S)S, \quad c_2(TY) \cdot D_7 = 2(3L - 2S)S, \\ Y_6 : \quad c_2(TY) \cdot D_5 &= 2(3L - 2S)S, \quad c_2(TY) \cdot D_7 = 2(7L - 5S)S, \\ Y_8 : \quad c_2(TY) \cdot D_4 &= 2(7L - 5S)S. \end{aligned}$$

Proof. The Chern class of the variety Y is computed using Theorem 5.3 and the rest follows from the pushforward results in Theorem 5.4 (or Theorem 5.6) and Theorem 5.5. \square

The characteristic numbers that we are interested in are

$$\tau(D) = \frac{1}{3} \int_D (-2c_2 + c_1^2) \quad \chi(D) = \int_D c_2, \quad \chi_0(D) = \int_D \frac{c_1^2 + c_2}{12}, \quad (7.1)$$

where $\tau(D)$ is the signature, $\chi(D)$ is its Euler number, and $\chi_0(D)$ is its holomorphic Euler characteristic.

Lemma 7.2. *Let D be a ruled surface over a smooth curve of genus g . Then*

$$\chi(D) = 4(1 - g), \quad \chi_0(D) = (1 - g), \quad \tau(D) = 0. \quad (7.2)$$

While the holomorphic Euler characteristic of a fibral divisor is the same for any crepant resolution, both the signature and the ordinary Euler characteristic depend on the choice of minimal model. We can use the Euler characteristic and the signature to identify fibral divisors that have reducible singular fibers. For instance, the signature is zero when the fibral divisor is a ruled variety.

Theorem 7.3. *The characteristic numbers of the fibral divisors of the crepant resolution of an E_7 -model are as follows for the relative minimal model Y_4 , Y_5 , Y_6 , and Y_8 :*

$$Y_4 \begin{cases} \chi_0(D_a) = (1 - g), & a = 0, 1, 2, 3, 4, 5, 6, 7 \\ \tau(D_a) = 0, & \chi(D_a) = 4(1 - g), & a = 0, 1, 2, 4, 5, 7 \\ \tau(D_3) = (4L - 3S)S, & \chi(D_3) = 4(1 - g) + (4L - 3S)S, \\ \tau(D_6) = 2(4L - 3S)S, & \chi(D_6) = 4(1 - g) + 2(4L - 3S)S, \end{cases} \quad (7.3)$$

$$Y_5 \begin{cases} \chi_0(D_a) = (1 - g), & a = 0, 1, 2, 3, 4, 5, 6, 7 \\ \tau(D_a) = 0, & \chi(D_a) = 4(1 - g), & a = 0, 1, 2, 3, 5 \\ \tau(D_a) = (4L - 3S)S, & \chi(D_a) = 4(1 - g) + (4L - 3S)S, & a = 4, 6, 7 \end{cases} \quad (7.4)$$

$$Y_6 \begin{cases} \chi_0(D_a) = (1 - g), & a = 0, 1, 2, 3, 4, 5, 6, 7 \\ \tau(D_a) = 0, & \chi(D_a) = 4(1 - g), & a = 0, 1, 2, 3, 4, 6 \\ \tau(D_5) = (4L - 3S)S, & \chi(D_5) = 4(1 - g) + (4L - 3S)S, \\ \tau(D_7) = 2(4L - 3S)S, & \chi(D_7) = 4(1 - g) + 2(4L - 3S)S, \end{cases} \quad (7.5)$$

$$Y_8 \begin{cases} \chi_0(D_a) = (1 - g), & a = 0, 1, 2, 3, 4, 5, 6, 7 \\ \tau(D_a) = 0, & \chi(D_a) = 4(1 - g), & a = 0, 1, 2, 3, 5, 6, 7 \\ \tau(D_4) = 2(4L - 3S)S, & \chi(D_4) = 4(1 - g) + 2(4L - 3S)S. \end{cases} \quad (7.6)$$

Proof. To ease the notation, we will not write all of the pushforwards and pullbacks. The total Chern class of a fibral divisor D is computed by adjoint from the total Chern class of the variety Y which, in turn, can be deduced from Theorem 5.3. Namely,

$$c(TD) = \frac{c(TY)}{1 + D} = 1 + (c_1(TY) - D) + (c_2(TY) - c_1(TY)D + D^2) + \dots \quad (7.7)$$

By adjoint for Y , we have

$$c_1(TY) = c_1(TB) - c_1(\mathcal{L}), \quad (7.8)$$

so we deduce that

$$c_1(TD) = c_1(TB) - L - D, \quad c_2(TD) = c_2(TY) - (c_1(TB) - L)D + D^2. \quad (7.9)$$

The second Chern class of Y will appear multiplied by the class of a fibral divisor and we can therefore use Theorem 7.1 to express all the results as functions of the base, once we pushforward to the base using Theorem 5.4 (or Theorem 5.6) and Theorem 5.5. \square

8 Fat fibers and loss of flatness

For a base of high enough dimension, there can be points over which the fiber is not a collection of rational curves, but rather contains an entire rational surface as a component. This phenomena has been studied in the case of an E_6 -model by analyzing a partial resolution of its Weierstrass model in [10]. In M-theory compactifications, the presence of a complex surface Q in the fiber results in new light degrees of freedom in the low energy spectrum, as M5-branes wrapping the surface can produce massless stringy modes and a tower of particle states arise by wrapping membranes on holomorphic curves in Q .

When the base of an E_7 -model has dimension three or higher, the fibration is no longer flat. When the locus $s = a = b = 0$ is non-empty, the divisor D_6 has a fiber over the divisor S that jumps in dimension to become a rational surface over this locus. In the minimal model Y_a , we call this rational surface Q_a . For the minimal models that are constructed explicitly by a crepant resolution, namely Y_a , ($a = 4, 5, 6, 8$), we can identify Q_a up to isomorphism, explicitly.

Theorem 8.1. *Let Y_a ($a = 1, \dots, 8$) be a crepant resolution of an E_7 -model with fibral divisors D_n with generic fibers C_n ($n = 0, \dots, 7$). Let Q_a be the surface that the fiber C_6 degenerates into over the locus $V(a, b) \cap S$. Then for Y_4 , Y_5 , Y_6 , and Y_8 , which can be defined by the crepant resolutions given in equation (4.1), we have:*

$$Q_4 \cong \mathbb{F}_2^{(2)}, \quad Q_5 \cong \mathbb{F}_1^{(1)}, \quad Q_6 \cong \mathbb{F}_1, \quad Q_8 \cong \mathbb{F}_2. \quad (8.1)$$

- Y_8 : The surface Q_8 is isomorphic to the Hirzebruch surface \mathbb{F}_2 .
- Y_6 : The surface Q_6 is isomorphic to an \mathbb{F}_1 (which is also a del Pezzo surface of degree 8).
- Y_5 : The surface Q_5 is a Hirzebruch surface \mathbb{F}_1 blown-up at a point of its curve of self-intersection -1 .
- Y_4 : The surface Q_4 is the blowup of a Hirzebruch surface \mathbb{F}_2 over a point p of the curve of self-intersection 2 followed by a blowup of the intersection point between the proper transform of that curve and the proper transform of the fiber over the point p . The structures of these rational surfaces are summarized in Figure 8.

The relevant computations can be found in Appendix D. Using adjunction, we compute the total Chern class of the surface Q and its characteristic numbers. We can then use this data to identify the surfaces.

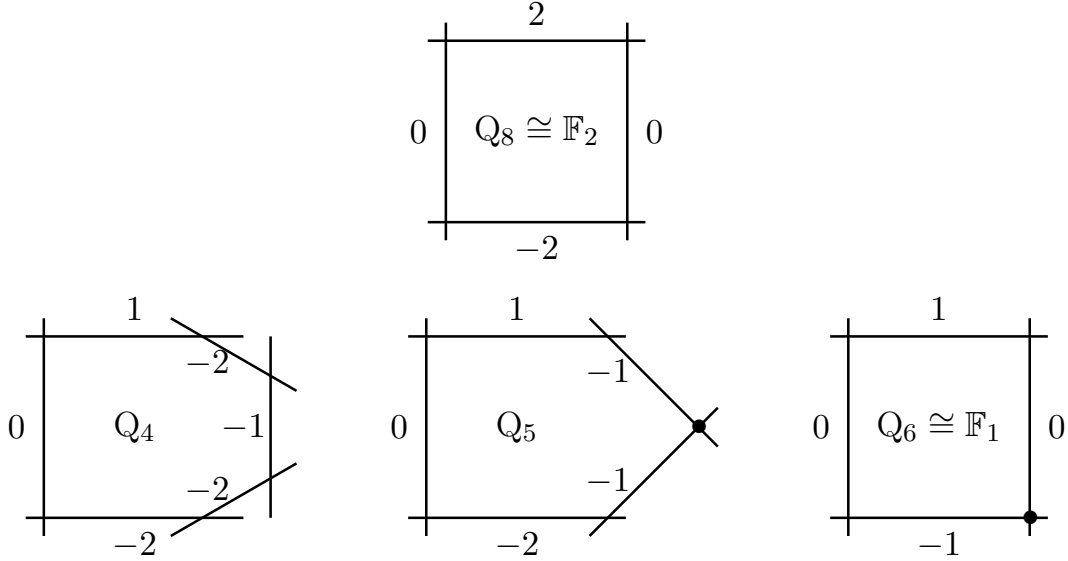


Figure 8: Isomorphism classes of the rational surfaces Q_a ($a = 4, 5, 6, 8$). For the crepant resolution Y_a , the fibral divisor D_6 has a generic fiber C_6 that degenerates into a full rational surface Q_a over the codimension-three locus $V(a, b) \cap S$. The four rational surfaces Q_a are connected to each other by blowing-up points or blowing-down (-1) -curves. The rational surfaces Q_8 and Q_6 are, respectively, isomorphic to the Hirzebruch surfaces \mathbb{F}_2 and \mathbb{F}_1 . The rational surface Q_5 is obtained by blowing-up a point of the (-1) -curve of \mathbb{F}_1 or by blowing-up a point of the curve of self-intersection 2 in \mathbb{F}_2 . Alternatively, Q_8 is obtained from Q_5 by contracting the (-1) -curve that is the proper transform of the fiber over the point p that was blown-up to go from Q_6 to Q_5 . The rational surface Q_4 is obtained by blowing-up the intersection of the two (-1) -curves of Q_5 .

Lemma 8.2. *The Euler characteristic, the degree, the holomorphic Euler characteristic, and signature of the surfaces Q_a ($a = 4, 5, 6, 8$) are:*

$$\begin{aligned}
Y_4: \quad & \chi(Q_4) = 6 \quad K_{Q_4}^2 = 6, \quad \chi_0(Q_4) = 1, \quad \tau(Q_4) = -2, \\
Y_5: \quad & \chi(Q_5) = 5 \quad K_{Q_5}^2 = 7, \quad \chi_0(Q_5) = 1, \quad \tau(Q_5) = -1, \\
Y_6: \quad & \chi(Q_6) = 4 \quad K_{Q_6}^2 = 8, \quad \chi_0(Q_6) = 1, \quad \tau(Q_6) = 0, \\
Y_8: \quad & \chi(Q_8) = 4 \quad K_{Q_8}^2 = 8, \quad \chi_0(Q_8) = 1, \quad \tau(Q_8) = 0.
\end{aligned}$$

While flops do not change the fibral divisor (namely D_6) whose generic fiber degenerates into the surface Q over $V(a, b, s)$, flops do change the topology of Q by blowing-up/down certain points. Such blowups will change $\chi(Q)$, K_Q^2 , and $\tau(Q)$. Since we know the degeneration of the fiber C_6 , we make the following conjectures.

Conjecture 8.1. *The Euler characteristic, the degree, the holomorphic Euler characteristic, and signature of the surfaces Q_a ($a = 1, 2, 3, 7$) are expected to be:*

$$\begin{aligned}
Y_1 : \quad & \chi(Q_1) = 9 \quad K_{Q_1}^2 = 3, \quad \chi_0(Q_1) = 1, \quad \tau(Q_1) = -5, \\
Y_2 : \quad & \chi(Q_2) = 8 \quad K_{Q_2}^2 = 4, \quad \chi_0(Q_2) = 1, \quad \tau(Q_2) = -4, \\
Y_3 : \quad & \chi(Q_3) = 7 \quad K_{Q_3}^2 = 5, \quad \chi_0(Q_3) = 1, \quad \tau(Q_3) = -3, \\
Y_7 : \quad & \chi(Q_7) = 4 \quad K_{Q_7}^2 = 8, \quad \chi_0(Q_7) = 1, \quad \tau(Q_7) = 0,
\end{aligned}$$

We expect Q_7 to be a Hirzebruch surface \mathbb{F}_1 , and Q_3 , Q_2 , and Q_1 to be the blowup of a Hirzebruch surface \mathbb{F}_2 at three, four, and five points, respectively. These points are on the fiber of self-intersection -2 and then on successive intersections of the proper transform of this fiber with the exceptional divisors.

A Fiber degenerations

Here we derive in detail the splitting of curves in each of the eight chambers using the hyperplane arrangement $I(E_7, \mathbf{56})$.

A.1 Ch_1

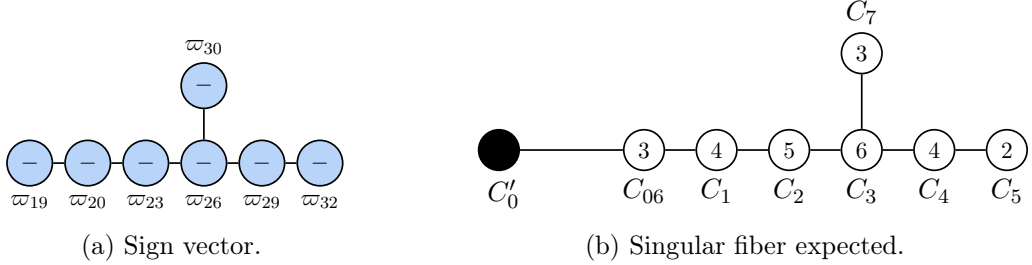


Figure 9: Chamber 1.

As we can see from Figure 4, the unique wall of chamber 1 that intersects the interior of the fundamental open Weyl chamber is the hyperplane ϖ_{19}^\perp . This hyperplane separates chamber 1 and chamber 2: the form $\langle \varpi_{19}, \phi \rangle$ is negative in the interior of the chamber 1, vanishes on the wall ϖ_{19}^\perp and is positive in chamber 2. The condition

$$\langle \varpi_{19}, \phi \rangle = \phi_1 - \phi_6 < 0, \quad (\text{A.1})$$

completely characterizes chamber 1 since ϖ_{19} is higher than all the other weights appearing in the sign vector. It follows that $-\varpi_{19}$ (resp. ϖ_{19}) is an effective curve in chamber 1 (resp. in chamber 2) which we call C'_6 .

Geometrically, any simple root is an effective curve in a given chamber unless it connects two weights of different signs. In the basis of simple roots, we have $\varpi_{19} = (1, 1, 1, \frac{1}{2}, 0, -\frac{1}{2}, \frac{1}{2})$ as listed in equation (3.1), or equivalently

$$\varpi_{19} = \alpha_1 + \alpha_2 + \alpha_3 + \frac{1}{2}\alpha_4 - \frac{1}{2}\alpha_6 + \frac{1}{2}\alpha_7. \quad (\text{A.2})$$

We rewrite this equation in the following suggestive form

$$\alpha_6 = 2(-\varpi_{19}) + 2\alpha_1 + 2\alpha_2 + 2\alpha_3 + \alpha_4 + \alpha_7 \quad (\text{A.3})$$

and deduce that the curve C_6 splits as follows:

$$C_6 \rightarrow 2C'_6 + 2C_1 + 2C_2 + 2C_3 + C_4 + C_7. \quad (\text{A.4})$$

This matches the description in [12]. The intersection number of C'_6 with the fibral divisor D_i is given by minus the coefficient of ϖ_{19} written in the basis of fundamental weights. Since in the basis of fundamental weights, we have $-(\varpi_{19}) = \boxed{1 \ 0 \ 0 \ 0 \ 0 \ -1 \ 0}$, we find

$$D_1 \cdot C'_6 = 1, \quad D_6 \cdot C'_6 = -1, \quad D_i \cdot C'_6 = 0, \quad i = 2, 3, 4, 5, 7. \quad (\text{A.5})$$

We also note that by linearity (see equation (3.2)), we have

$$D_0 \cdot C'_6 = -1, \quad (\text{A.6})$$

which is negative and therefore implies that D_0 contains C'_6 . Since both D_0 and D_6 contain C'_6 , we rename C'_6 as C_{06} and we have the splitting rule

$$\begin{cases} C_0 \rightarrow C_{06} + C'_0 \\ C_6 \rightarrow 2C_{06} + 2C_1 + 2C_2 + 2C_3 + C_4 + C_7 \end{cases} \quad (\text{A.7})$$

where C'_0 is the left-over curve in C_0 . Since C_0 has weight ϖ_0 and C_{06} has weight $-\varpi_{19}$, and $\varpi_0 = -\varpi_{19} - \varpi_1$, we see that $-\varpi_1$ is the weight of C'_0 :

$$\begin{cases} C_{06} \rightarrow -\varpi_{19}, \\ C'_0 \rightarrow \boxed{0 \ 0 \ 0 \ 0 \ 0 \ -1 \ 0} = -\varpi_1. \end{cases} \quad (\text{A.8})$$

From the Dynkin indices of ϖ_1 , we deduce the following intersection numbers

$$D_0 \cdot C'_0 = -1, \quad D_r \cdot C'_0 = 0 \quad r = 1, 2, 3, 4, 5, 7, \quad D_6 \cdot C'_0 = 1, \quad (\text{A.9})$$

and the degeneration

$$C_0 + 2C_1 + 3C_2 + 4C_3 + 3C_4 + 2C_5 + C_6 + 2C_7 \rightarrow C'_0 + 3C_{06} + 4C_1 + 5C_2 + 6C_3 + 4C_4 + 2C_5 + 3C_7 \quad (\text{A.10})$$

We get a fiber whose dual graph is the affine Dynkin diagram \tilde{E}_8 with the node corresponding to α_1 contracted to a point and the identification:

$$(C'_0, C_{06}, C_1, C_2, C_3, C_4, C_5, C_7) \rightarrow (\alpha_0, \alpha_2, \alpha_3, \alpha_4, \alpha_5, \alpha_6, \alpha_7, \alpha_8), \quad (\text{A.11})$$

with the respective multiplicities $(1, 3, 4, 5, 6, 4, 2, 3)$.

A.2 Ch_2

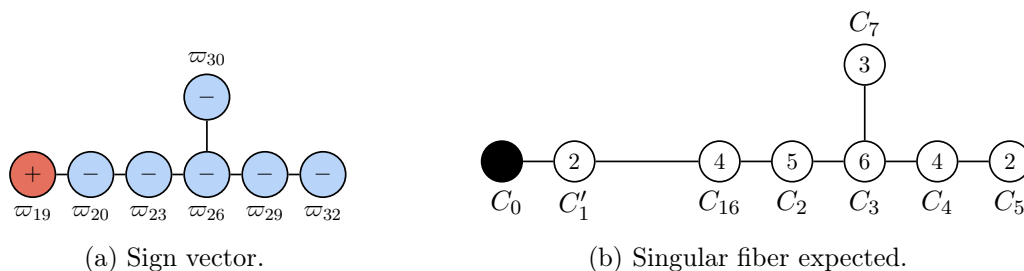


Figure 10: Chamber 2.

In chamber 2, we see from Figure 4 that the extremal faces are ϖ_{19}^\perp and ϖ_{20}^\perp with

$$\varpi_{19} - \alpha_1 = \varpi_{20}, \quad \varpi_{19} \cdot \phi > 0, \quad \varpi_{20} \cdot \phi < 0. \quad (\text{A.12})$$

We conclude that ϖ_{19} and $-\varpi_{20}$ will correspond to effective extremal curves in this chamber. We can also use the expression of ϖ_{20} in terms of simple roots:

$$\varpi_{19} = \alpha_1 + \alpha_2 + \alpha_3 + \frac{1}{2}\alpha_4 - \frac{1}{2}\alpha_6 + \frac{1}{2}\alpha_7, \quad \varpi_{20} = \alpha_2 + \alpha_3 + \frac{1}{2}\alpha_4 - \frac{1}{2}\alpha_6 + \frac{1}{2}\alpha_7 \quad (\text{A.13})$$

and solve for α_1 and α_6 as sums of weights that define a positive form in the interior of the chamber:

$$\alpha_1 = \varpi_{19} + (-\varpi_{20}), \quad \alpha_6 = 2(-\varpi_{20}) + 2\alpha_2 + 2\alpha_3 + \alpha_4 + \alpha_7. \quad (\text{A.14})$$

There is an effective curve C_{16} corresponding to $-\varpi_{20}$ and an effective curve C'_1 corresponding to ϖ_{19} . Our choice of notation is because $-\varpi_{20}$ shows up for both α_1 and α_6 while ϖ_{19} only appears in α_1 , which we see as follows.

Since in the basis of fundamental weights, we have $-(\varpi_{20}) = \boxed{-1 \ 1 \ 0 \ 0 \ 0 \ -1 \ 0}$, we deduce

$$D_1 \cdot C_{16} = -1, \quad D_2 \cdot C_{16} = 1, \quad D_6 \cdot C_{16} = -1, \quad D_i \cdot C_{16} = 0, \quad i = 3, 4, 5, 7. \quad (\text{A.15})$$

We also note that by linearity

$$D_0 \cdot C_{16} = 0. \quad (\text{A.16})$$

The negative intersection numbers imply both D_1 and D_6 contain C_{16} . Meanwhile from $-(\varpi_{19}) = \boxed{-1 \ 0 \ 0 \ 0 \ 0 \ 1 \ 0}$, we deduce the intersections of C'_1 which are the negative of those computed for C_{06} above, namely

$$D_0 \cdot C'_6 = 1, \quad D_1 \cdot C'_6 = -1, \quad D_6 \cdot C'_6 = 1, \quad D_i \cdot C'_6 = 0, \quad i = 2, 3, 4, 5, 7. \quad (\text{A.17})$$

We then have

$$\begin{cases} C_1 \rightarrow C_{16} + C'_1 \\ C_6 \rightarrow 2C_{16} + 2C_2 + 2C_3 + C_4 + C_7. \end{cases} \quad (\text{A.18})$$

Using these linear equations, we find:

$$C_0 + 2C_1 + 3C_2 + 4C_3 + 3C_5 + C_6 + 2C_7 \rightarrow 2C'_1 + 4C_{16} + 5C_2 + 6C_3 + 4C_4 + 2C_5 + 3C_7. \quad (\text{A.19})$$

We get a fiber whose dual graph is the affine Dynkin diagram \tilde{E}_8 with the node corresponding to α_2 contracted to a point and the identification:

$$(C_0, C'_1, C_{16}, C_1, C_2, C_3, C_4, C_5, C_7) \rightarrow (\alpha_0, \alpha_1, \alpha_3, \alpha_4, \alpha_5, \alpha_6, \alpha_7, \alpha_8), \quad (\text{A.20})$$

with the respective multiplicities $(1, 2, 4, 5, 6, 4, 2, 3)$.

A.3 Ch₃

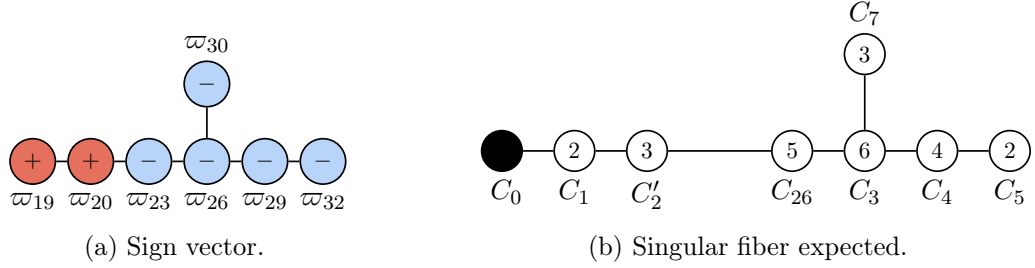


Figure 11: Chamber 3.

The interior walls are now ϖ_{20} and ϖ_{23} with

$$\varpi_{20} - \alpha_2 = \varpi_{23}, \quad \varpi_{20} \cdot \phi > 0, \quad \varpi_{23} \cdot \phi < 0. \quad (\text{A.21})$$

We conclude that ϖ_{20} and $-\varpi_{23}$ will correspond to effective extremal curves in this chamber. We can also use the expressions for these weights in terms of simple roots:

$$\begin{cases} \varpi_{20} = \alpha_2 + \alpha_3 + \frac{1}{2}\alpha_4 - \frac{1}{2}\alpha_6 + \frac{1}{2}\alpha_7, \\ \varpi_{23} = \alpha_3 + \frac{1}{2}\alpha_4 - \frac{1}{2}\alpha_6 + \frac{1}{2}\alpha_7. \end{cases} \quad (\text{A.22})$$

Solving for α_2 and α_6 , we have

$$\alpha_2 = \varpi_{20} + (-\varpi_{23}), \quad \alpha_6 = 2(-\varpi_{20}) + 2\alpha_3 + \alpha_4 + \alpha_7. \quad (\text{A.23})$$

There is an effective curve C_{26} corresponding to $-\varpi_{23}$ and an effective curve C'_2 corresponding to ϖ_{20} . We thus have

$$\begin{cases} C_2 \rightarrow C_{26} + C'_2 \\ C_6 \rightarrow 2C_{26} + 2C_3 + C_4 + C_7. \end{cases} \quad (\text{A.24})$$

Our choice of notation is because C_{26} shows up for both α_2 and α_6 while C'_2 only appears in α_2 , which we see as follows.

Since in the basis of fundamental weights, we have $-(-\varpi_{23}) = \boxed{0 \ -1 \ 1 \ 0 \ 0 \ -1 \ 0}$, we deduce

$$D_2 \cdot C_{26} = -1, \quad D_3 \cdot C_{26} = 1, \quad D_6 \cdot C_{26} = -1, \quad D_i \cdot C_{26} = 0, \quad i = 1, 4, 5, 7. \quad (\text{A.25})$$

We also note that by linearity $D_0 \cong -(2D_1 + 3D_2 + 4D_3 + 3D_4 + 2D_5 + D_6 + 2D_7)$, hence,

$$D_0 \cdot C_{26} = 0. \quad (\text{A.26})$$

The negative intersection numbers imply both D_2 and D_6 contain C_{26} . Meanwhile from $-(\varpi_{20}) = \boxed{1 \ -1 \ 0 \ 0 \ 1 \ 0}$, we deduce the intersections of C'_2 which are the negative of those computed for C_{16} above, namely

$$D_1 \cdot C'_2 = 1, \quad D_2 \cdot C'_2 = -1, \quad D_6 \cdot C'_2 = 1, \quad D_i \cdot C'_2 = 0, \quad i = 0, 3, 4, 5, 7. \quad (\text{A.27})$$

Finally we find the degeneration

$$C_0 + 2C_1 + 3C_2 + 4C_3 + 3C_4 + 2C_5 + C_6 + 2C_7 \rightarrow C_0 + 2C_1 + 3C'_2 + 5C_{26} + 6C_3 + 4C_4 + 2C_5 + 3C_7. \quad (\text{A.28})$$

We get a fiber whose dual graph is the affine Dynkin diagram \tilde{E}_8 with the node corresponding to α_3 contracted to a point and the identification:

$$(C_0, C_1, C'_2, C_{26}, C_3, C_4, C_5, C_7) \rightarrow (\alpha_0, \alpha_1, \alpha_2, \alpha_4, \alpha_5, \alpha_6, \alpha_7, \alpha_8), \quad (\text{A.29})$$

with the respective multiplicities $(1, 2, 3, 5, 6, 4, 2, 3)$.

A.4 Ch_4

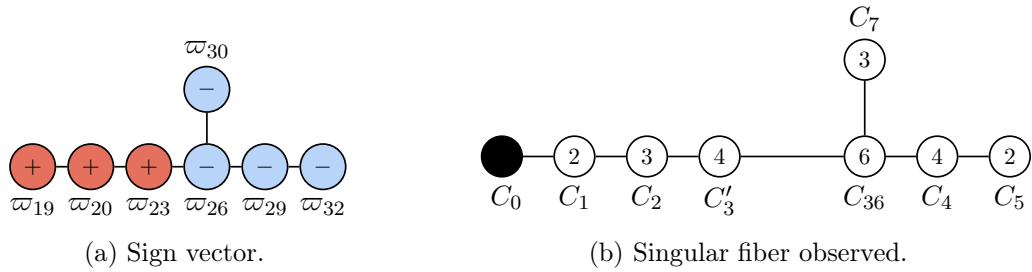


Figure 12: Chamber 4.

The interior walls are now ϖ_{23} and ϖ_{26} with

$$\varpi_{23} - \alpha_3 = \varpi_{26}, \quad \varpi_{23} \cdot \phi > 0, \quad \varpi_{26} \cdot \phi < 0. \quad (\text{A.30})$$

We conclude that ϖ_{23} and $-\varpi_{26}$ will correspond to effective extremal curves in this chamber. We can also use the expressions for these weights in terms of simple roots:

$$\begin{cases} \varpi_{23} = \alpha_3 + \frac{1}{2}\alpha_4 - \frac{1}{2}\alpha_6 + \frac{1}{2}\alpha_7, \\ \varpi_{26} = \frac{1}{2}\alpha_4 - \frac{1}{2}\alpha_6 + \frac{1}{2}\alpha_7. \end{cases} \quad (\text{A.31})$$

Solving for α_3 and α_6 , we have

$$\alpha_3 = \varpi_{23} + (-\varpi_{26}), \quad \alpha_6 = 2(-\varpi_{26}) + \alpha_4 + \alpha_7. \quad (\text{A.32})$$

There is an effective curve C_{36} corresponding to $-\varpi_{26}$ and an effective curve C'_3 corresponding to ϖ_{23} . We thus have

$$\begin{cases} C_3 \rightarrow C_{36} + C'_3 \\ C_6 \rightarrow 2C_{36} + C_4 + C_7. \end{cases} \quad (\text{A.33})$$

Our choice of notation is because C_{36} shows up for both α_3 and α_6 while C'_3 only appears in α_3 , which we see as follows. Since in the basis of fundamental weights, we have $-(\varpi_{26}) = \boxed{0 \ 0 \ -1 \ 1 \ 0 \ -1 \ 1}$, we deduce

$$D_3 \cdot C_{36} = -1, \quad D_4 \cdot C_{36} = 1, \quad D_6 \cdot C_{36} = -1, \quad D_7 \cdot C_{36} = 1, \quad D_i \cdot C_{26} = 0, \quad i = 1, 2, 5. \quad (\text{A.34})$$

We also note that by linearity $D_0 \cong -(2D_1 + 3D_2 + 4D_3 + 3D_4 + 2D_5 + D_6 + 2D_7)$, hence,

$$D_0 \cdot C_{36} = 0. \quad (\text{A.35})$$

The negative intersection numbers imply both D_3 and D_6 contain C_{36} . Meanwhile from $-(\varpi_{23}) = \begin{bmatrix} 0 & 1 & -1 & 0 & 0 & 1 & 0 \end{bmatrix}$, we deduce the intersections of C'_3 which are the negative of those computed for C_{26} above. Namely,

$$D_2 \cdot C'_3 = -1, \quad D_3 \cdot C'_3 = 1, \quad D_6 \cdot C'_3 = -1, \quad D_i \cdot C'_3 = 0, \quad i = 0, 1, 4, 5, 7. \quad (\text{A.36})$$

Finally we find the degeneration

$$C_0 + 2C_1 + 3C_2 + 4C_3 + 3C_4 + 2C_5 + C_6 + 2C_7 \rightarrow C_0 + 2C_1 + 3C_2 + 4C'_3 + 6C_{36} + 4C_4 + 2C_5 + 3C_7. \quad (\text{A.37})$$

We get a fiber whose dual graph is the affine Dynkin diagram \tilde{E}_8 with the node corresponding to α_4 contracted to a point and the identification:

$$(C_0, C_1, C_2, C'_3, C_{36}, C_4, C_5, C_7) \rightarrow (\alpha_0, \alpha_1, \alpha_2, \alpha_4, \alpha_5, \alpha_6, \alpha_7, \alpha_8), \quad (\text{A.38})$$

with the respective multiplicities $(1, 2, 3, 4, 6, 4, 2, 3)$.

A.5 Ch₅

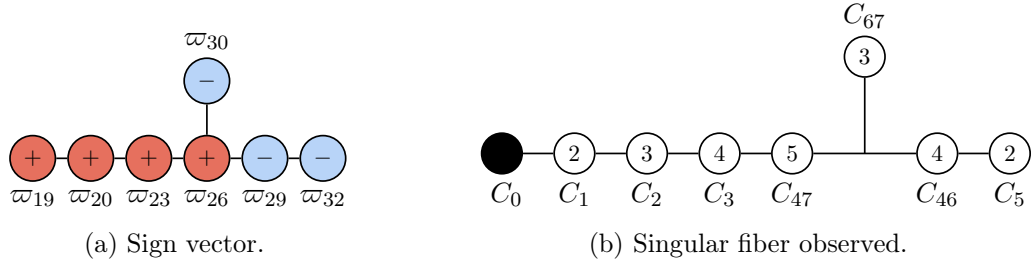


Figure 13: Chamber 5.

The interior walls are now ϖ_{26} , ϖ_{29} , and ϖ_{30} with

$$\varpi_{26} - \alpha_4 = \varpi_{29}, \quad \varpi_{26} - \alpha_7 = \varpi_{30}, \quad \varpi_{26} \cdot \phi > 0, \quad \varpi_{29} \cdot \phi < 0, \quad \varpi_{30} \cdot \phi < 0. \quad (\text{A.39})$$

We conclude that ϖ_{26} , $-\varpi_{29}$, and $-\varpi_{30}$ will correspond to effective extremal curves in this chamber. We can also use the expressions for these weights in terms of simple roots:

$$\begin{cases} \varpi_{26} = \frac{1}{2}\alpha_4 - \frac{1}{2}\alpha_6 + \frac{1}{2}\alpha_7, \\ \varpi_{29} = -\frac{1}{2}\alpha_4 - \frac{1}{2}\alpha_6 + \frac{1}{2}\alpha_7, \\ \varpi_{30} = \frac{1}{2}\alpha_4 - \frac{1}{2}\alpha_6 - \frac{1}{2}\alpha_7. \end{cases} \quad (\text{A.40})$$

Solving for α_4 , α_6 , and α_7 we have

$$\alpha_4 = \varpi_{26} + (-\varpi_{29}), \quad \alpha_7 = \varpi_{26} + (-\varpi_{30}), \quad \alpha_6 = (-\varpi_{29}) + (-\varpi_{30}). \quad (\text{A.41})$$

There is an effective curve C_{47} corresponding to ϖ_{26} , an effective curve C_{46} corresponding to $-\varpi_{29}$, and an effective curve C_{67} corresponding to $-\varpi_{30}$. We thus have

$$\begin{cases} C_4 \rightarrow C_{46} + C_{47}, \\ C_6 \rightarrow C_{46} + C_{67}, \\ C_7 \rightarrow C_{47} + C_{67}. \end{cases} \quad (\text{A.42})$$

Our choice of notation is because C_{46} shows up for both α_4 and α_6 , C_{47} shows up for both α_4 and α_7 , and C_{67} shows up for both α_6 and α_7 , which we see as follows. Since in the basis of fundamental weights, we have $-(\varpi_{26}) = \boxed{0 \ 0 \ 1 \ -1 \ 0 \ 1 \ -1}$, we deduce

$$D_3 \cdot C_{47} = 1, \quad D_4 \cdot C_{47} = -1, \quad D_6 \cdot C_{47} = 1, \quad D_7 \cdot C_{47} = -1, \quad D_i \cdot C_{26} = 0, \quad i = 0, 1, 2, 5.$$

The negative intersection numbers imply both D_4 and D_7 contain C_{47} . Meanwhile, from $-(-\varpi_{29}) = \boxed{0 \ 0 \ 0 \ -1 \ 1 \ -1 \ 1}$, we deduce

$$D_4 \cdot C_{46} = -1, \quad D_5 \cdot C_{46} = 1, \quad D_6 \cdot C_{46} = -1, \quad D_7 \cdot C_{46} = 1, \quad D_i \cdot C_{57} = 0, \quad i = 0, 1, 2, 3.$$

The negative intersection numbers imply both D_4 and D_6 contain C_{46} . Finally, from $-(-\varpi_{30}) = \boxed{0 \ 0 \ 0 \ 1 \ 0 \ -1 \ -1}$, we deduce

$$D_4 \cdot C_{67} = 1, \quad D_6 \cdot C_{67} = -1, \quad D_7 \cdot C_{67} = -1, \quad D_i \cdot C'_5 = 0, \quad i = 0, 1, 2, 3, 5$$

and the negative intersection numbers imply both D_6 and D_7 contain C_{67} .

In the end, we find the degeneration

$$C_0 + 2C_1 + 3C_2 + 4C_3 + 3C_4 + 2C_5 + C_6 + 2C_7 \rightarrow C_0 + 2C_1 + 3C_2 + 4C_3 + 5C_{47} + 4C_{46} + 2C_5 + 3C_{67}.$$

We get a fiber whose dual graph is the affine Dynkin diagram \tilde{E}_8 with the node corresponding to α_5 contracted to a point and the identification:

$$(C_0, C_1, C_2, C_3, C_{47}, C_{46}, C_5, C_{67}) \rightarrow (\alpha_0, \alpha_1, \alpha_2, \alpha_3, \alpha_4, \alpha_6, \alpha_7, \alpha_8),$$

with the respective multiplicities $(1, 2, 3, 4, 6, 4, 2, 3)$.

A.6 Ch₆

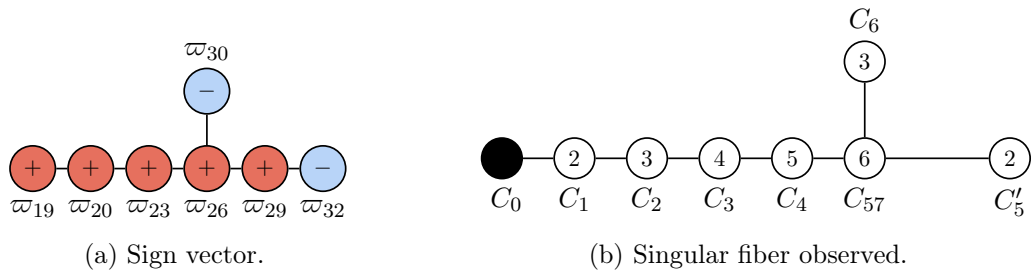


Figure 14: Chamber 6.

The interior walls are now ϖ_{29} and ϖ_{32} with

$$\varpi_{29} - \alpha_5 = \varpi_{32}, \quad \varpi_{29} \cdot \phi > 0, \quad \varpi_{32} \cdot \phi < 0. \quad (\text{A.43})$$

We conclude that ϖ_{29} and $-\varpi_{32}$ will correspond to effective extremal curves in this chamber. We can also use the expressions for these in terms of simple roots:

$$\begin{cases} \varpi_{29} = -\frac{1}{2}\alpha_4 - \frac{1}{2}\alpha_6 + \frac{1}{2}\alpha_7, \\ \varpi_{32} = -\frac{1}{2}\alpha_4 - \alpha_5 - \frac{1}{2}\alpha_6 + \frac{1}{2}\alpha_7. \end{cases} \quad (\text{A.44})$$

Solving for α_5 and α_7 , we have

$$\alpha_5 = \varpi_{29} + (-\varpi_{32}), \quad \alpha_7 = 2\varpi_{29} + \alpha_4 + \alpha_6. \quad (\text{A.45})$$

There is an effective curve C_{57} corresponding to ϖ_{29} and an effective curve C'_5 corresponding to $-\varpi_{32}$. We thus have

$$\begin{cases} C_5 \rightarrow C_{57} + C'_5 \\ C_7 \rightarrow 2C_{57} + C_4 + C_6. \end{cases} \quad (\text{A.46})$$

Since in the basis of fundamental weights, we have $-(\varpi_{29}) = \boxed{0 \ 0 \ 0 \ 1 \ -1 \ 1 \ -1}$, we deduce

$$D_4 \cdot C_{57} = 1, \quad D_5 \cdot C_{57} = -1, \quad D_6 \cdot C_{57} = 1, \quad D_7 \cdot C_{57} = -1, \quad D_i \cdot C_{57} = 0, \quad i = 1, 2, 3. \quad (\text{A.47})$$

We also note that by linearity $D_0 \cong -(2D_1 + 3D_2 + 4D_3 + 3D_4 + 2D_5 + D_6 + 2D_7)$, hence,

$$D_0 \cdot C_{57} = 0. \quad (\text{A.48})$$

The negative intersection numbers imply both D_5 and D_7 contain C_{57} . Meanwhile from $-(-\varpi_{32}) = \boxed{0 \ 0 \ 0 \ 0 \ -1 \ 0 \ 1}$, we deduce the intersection of C'_5 , namely

$$D_5 \cdot C'_5 = -1, \quad D_7 \cdot C'_5 = 1, \quad D_i \cdot C'_5 = 0, \quad i = 1, 2, 3, 4, 6, \quad (\text{A.49})$$

and, by linearity,

$$D_0 \cdot C_{57} = 0. \quad (\text{A.50})$$

Finally we find the degeneration

$$C_0 + 2C_1 + 3C_2 + 4C_3 + 3C_4 + 2C_5 + C_6 + 2C_7 \rightarrow C_0 + 2C_1 + 3C_2 + 4C_3 + 5C_4 + 6C_{57} + 2C'_5 + 3C_6. \quad (\text{A.51})$$

We get a fiber whose dual graph is the affine Dynkin diagram \tilde{E}_8 with the node corresponding to α_6 contracted to a point and the identification:

$$(C_0, C_1, C_2, C_3, C_4, C_{57}, C'_5, C_6) \rightarrow (\alpha_0, \alpha_1, \alpha_2, \alpha_3, \alpha_4, \alpha_5, \alpha_7, \alpha_8), \quad (\text{A.52})$$

with the respective multiplicities $(1, 2, 3, 4, 5, 6, 2, 3)$.

A.7 Ch₇

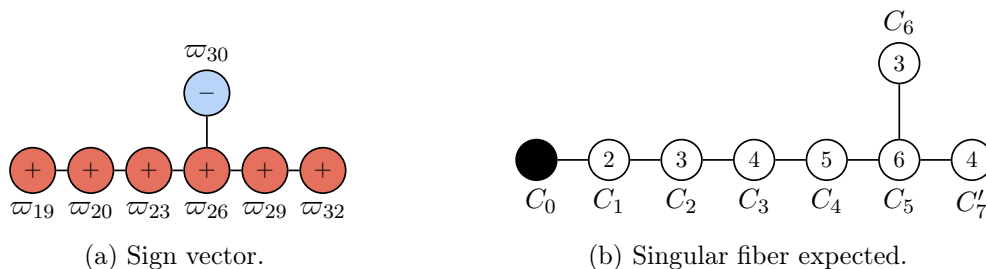


Figure 15: Chamber 7.

The interior wall is now ϖ_{32} with

$$\varpi_{32} \cdot \phi > 0. \quad (\text{A.53})$$

We conclude that ϖ_{32} will correspond to an effective extremal curve in this chamber. Recalling its expression in terms of simple roots:

$$\varpi_{32} = -\frac{1}{2}\alpha_4 - \alpha_5 - \frac{1}{2}\alpha_6 + \frac{1}{2}\alpha_7, \quad (\text{A.54})$$

we have

$$\alpha_7 = 2\varpi_{32} + \alpha_4 + 2\alpha_5 + \alpha_6. \quad (\text{A.55})$$

There is an effective curve C'_7 corresponding to ϖ_{32} , and we have

$$C_7 \rightarrow C_4 + 2C_5 + C_6 + 2C'_7. \quad (\text{A.56})$$

Since in the basis of fundamental weights, we have $-(\varpi_{32}) = \boxed{0 \ 0 \ 0 \ 0 \ 1 \ 0 \ -1}$, we deduce the intersections of C'_7 , namely

$$D_5 \cdot C'_7 = 1, \quad D_7 \cdot C'_7 = -1, \quad D_i \cdot C'_7 = 0, \quad i = 0, 1, 2, 3, 4, 6, \quad (\text{A.57})$$

which are the negative of those found for C'_5 in the previous chamber.

Finally, we find the degeneration

$$C_0 + 2C_1 + 3C_2 + 4C_3 + 3C_4 + 2C_5 + C_6 + 2C_7 \rightarrow C_0 + 2C_1 + 3C_2 + 4C_3 + 5C_4 + 6C_5 + 4C'_7 + 3C_6. \quad (\text{A.58})$$

We get a fiber whose dual graph is the affine Dynkin diagram \tilde{E}_8 with the node corresponding to α_7 contracted to a point and the identification:

$$(C_0, C_1, C_2, C_3, C_4, C_5, C'_7, C_6) \rightarrow (\alpha_0, \alpha_1, \alpha_2, \alpha_3, \alpha_4, \alpha_5, \alpha_6, \alpha_8), \quad (\text{A.59})$$

with the respective multiplicities $(1, 2, 3, 4, 5, 6, 4, 3)$.

A.8 Ch₈

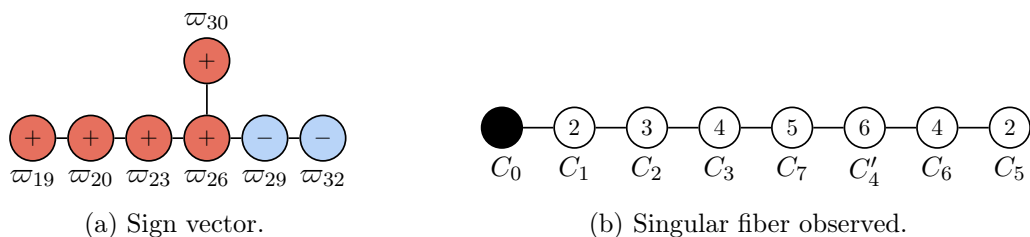


Figure 16: Chamber 8.

Chamber 8 is only adjacent to chamber 5 and the two chambers are separated by the hyperplane ϖ_{30}^\perp (as seen in Figure 4). In particular, chamber 8 is characterized by:

$$\varpi_{30} \cdot \phi = \phi_4 - \phi_6 - \phi_7 > 0. \quad (\text{A.60})$$

We conclude that in this chamber, the weight ϖ_{30} will correspond to an effective extremal curve. Recalling its expression in terms of simple roots:

$$\varpi_{30} = \frac{1}{2}\alpha_4 - \frac{1}{2}\alpha_6 - \frac{1}{2}\alpha_7, \quad (\text{A.61})$$

we have

$$\alpha_4 = 2\varpi_{30} + \alpha_6 + \alpha_7. \quad (\text{A.62})$$

There is an effective curve C'_4 corresponding to ϖ_{30} , and we have

$$C_4 \rightarrow C_6 + C_7 + 2C'_4. \quad (\text{A.63})$$

Since in the basis of fundamental weights, we have $-(\varpi_{30}) = \boxed{0 \ 0 \ 0 \ -1 \ 0 \ 1 \ 1}$, we deduce the intersections of C'_4 , namely

$$D_4 \cdot C'_4 = -1, \quad D_6 \cdot C'_4 = 1, \quad D_7 \cdot C'_4 = 1, \quad D_i \cdot C'_4 = 0, \quad i = 1, 2, 3, 5, \quad (\text{A.64})$$

and by linearity $D_0 \cong -(2D_1 + 3D_2 + 4D_3 + 3D_4 + 2D_5 + D_6 + 2D_7)$ hence,

$$D_0 \cdot C'_4 = 0. \quad (\text{A.65})$$

Finally we find the degeneration

$$C_0 + 2C_1 + 3C_2 + 4C_3 + 3C_4 + 2C_5 + C_6 + 2C_7 \rightarrow C_0 + 2C_1 + 3C_2 + 4C_3 + 5C_7 + 6C'_4 + 4C_6 + 2C_5. \quad (\text{A.66})$$

We get a fiber whose dual graph is the affine Dynkin diagram \tilde{E}_8 with the node corresponding to α_8 contracted to a point and the identification:

$$(C_0, C_1, C_2, C_3, C_7, C'_4, C_6, C_5) \rightarrow (\alpha_0, \alpha_1, \alpha_2, \alpha_3, \alpha_4, \alpha_5, \alpha_6, \alpha_7), \quad (\text{A.67})$$

with the respective multiplicities $(1, 2, 3, 4, 5, 6, 4, 2)$.

B Triple intersection computations

Here we compute the triple intersection polynomials in each chamber for which we have an explicit resolution of singularities.

B.1 Y_4

Y_4 is the proper transform of the Weierstrass model of equation (2.2) after the blowups leading to X_7'' in (4.1). The result is

$$Y_4 : \quad e_3 e_5 e_6 y^2 - e_1 e_2 e_4 (b e_1^2 e_3^2 e_4 e_6 e_7^2 s^5 + a e_1 e_3 s^3 x + e_2 e_5 x^3) = 0, \quad (\text{B.1})$$

where the relative projective coordinates are

$$\begin{aligned} & [e_2 e_4 e_5 e_6 e_7^2 x : e_2 e_3 e_4^2 e_5^2 e_6^3 e_7^5 y : s] [x : e_3 e_4 e_5 e_6^2 e_7^3 y : e_1 e_3 e_4 e_6 e_7^2] \\ & [e_5 e_6 e_7 y : e_1] [e_2 e_5 : e_3] [e_6 e_7 y : e_2] [y : e_4 e_7] [e_4 : e_6]. \end{aligned} \quad (\text{B.2})$$

The total transform of s is $s e_1 e_2 e_3 e_4^2 e_5 e_6^2 e_7^4$ and we have the following fibral divisors

$$\left\{ \begin{array}{l} 1 D_0 : \quad s = e_3 e_6 y^2 - e_1 e_2^2 e_4 x^3 = 0, \\ 2 D_1 : \quad e_1 = e_3 = 0, \\ 3 D_2 : \quad e_3 = e_4 = 0, \\ 4 D_3 : \quad e_7 = e_3 e_5 e_6 y^2 - e_1 e_2 e_4 (a e_1 e_3 s^3 x + e_2 e_5 x^3) = 0, \\ 3 D_4 : \quad e_4 = e_5 = 0, \\ 2 D_5 : \quad e_2 = e_5 = 0, \\ 1 D_6 : \quad e_5 = b e_1 e_3 e_4 e_6 e_7^2 s^2 + a x = 0, \\ 2 D_7 : \quad e_6 = a e_1 e_3 s^3 + e_2 e_5 x^2 = 0. \end{array} \right. \quad (\text{B.3})$$

The classes of the Cartier divisors defined by the zero loci of s, x, y, e_i ($i = 1, \dots, 7$) are

$$\left\{ \begin{array}{l} [s] = S - E_1, \quad [x] = H + 2L - E_1 - E_2, \quad [y] = H + 3L - E_1 - E_2 - E_3 - E_5 - E_6, \\ [e_1] = E_1 - E_2 - E_3, \quad [e_2] = E_2 - E_4 - E_5, \quad [e_3] = E_3 - E_4, \\ [e_4] = E_4 - E_6 - E_7, \quad [e_5] = E_5, \quad [e_6] = E_6 - E_7, \quad [e_7] = E_7, \end{array} \right. \quad (\text{B.4})$$

where E_i is the total transform of the i^{th} exceptional divisor and $[e_i]$ is the proper transform of the i^{th} exceptional divisor.

We have the linear relations

$$\begin{aligned} [e_1] &= D_1, \quad [e_2] = D_5, \quad [e_3] = D_1 + D_2, \quad [e_4] = D_2 + D_4, \\ [e_5] &= D_4 + D_5 + D_6, \quad [e_6] = D_7, \quad [e_7] = D_3, \end{aligned} \quad (\text{B.5})$$

and can thus solve for the D_i in terms of the E_i to get⁹

$$\begin{cases} D_0 = S - E_1, \\ D_1 = E_1 - E_2 - E_3, \\ D_2 = -E_1 + E_2 + 2E_3 - E_4, \\ D_3 = E_7, \\ D_4 = E_1 - E_2 - 2E_3 + 2E_4 - E_6 - E_7, \\ D_5 = E_2 - E_4 - E_5, \\ D_6 = -E_1 + 2E_3 - E_4 + 2E_5 + E_6 + E_7, \\ D_7 = E_6 - E_7. \end{cases} \quad (\text{B.6})$$

Now that we have the classes of the fibral divisors, the sequence of blowups and the pushforward theorems will be enough to compute the triple intersection numbers.

The triple intersection polynomial is by definition

$$F = \int \left(\sum_{a=0}^7 D_a \phi_a \right)^3 [Y] = \int_B \pi_* f_{1*} f_{2*} f_{3*} f_{4*} f_{5*} f_{6*} f_{7*} f_{8*} \left[\left(\sum_{a=0}^7 D_a \phi_a \right)^3 [Y] \right], \quad (\text{B.7})$$

where f_i is the i^{th} blowup and $\pi : X_0 = \mathbb{P}[\mathcal{O}_B \oplus \mathcal{L}^{\otimes 2} \oplus \mathcal{L}^{\otimes 3}] \rightarrow B$ is the map defining the projective bundle. Noting that

$$[Y_4] = 3H + 6L - 2E_1 - 2E_2 - E_3 - E_4 - E_5 - E_6 - E_7, \quad (\text{B.8})$$

we can use the pushforward theorems from Section 5 to get:

$$\begin{aligned} F_4(\phi) = & 4S(L - S)(\phi_0^3 + \phi_1^3 + \phi_2^3 + \phi_4^3 + \phi_5^3 + \phi_7^3) - S^2\phi_3^3 + 2S(S - 2L)\phi_6^3 \\ & + 3S(-2L + S)\phi_0^2\phi_1 + 3LS\phi_0\phi_1^2 + 3S(-3L + 2S)\phi_1^2\phi_2 + 3S(2L - S)\phi_1\phi_2^2 \\ & + 3S(3S - 4L)(\phi_3\phi_2^2 + \phi_3^2\phi_6 + \phi_3\phi_6^2 + 2\phi_4^2\phi_6 + 2\phi_6\phi_7^2) \\ & + 3S(3L - 2S)\phi_3^2\phi_2 + 3S(9S - 11L)\phi_5^2\phi_6 + 6S(5L - 4S)\phi_5\phi_6^2 \\ & + 3S(S - L)(\phi_3^2\phi_4 + \phi_3^2\phi_7 + 2\phi_4^2\phi_5 - \phi_4\phi_5^2) \\ & - 6S(3S - 4L)(\phi_3\phi_4\phi_6 + \phi_4\phi_5\phi_6 + \phi_3\phi_6\phi_7). \end{aligned} \quad (\text{B.9})$$

B.2 Y_5

Y_5 is the proper transform of the Weierstrass model of equation (2.2) after the blowups leading to X_7^+ in (4.1). The result is

$$Y_5 : \quad e_3e_5e_6y^2 - e_1e_2e_4(be_1^2e_3^2e_4e_5e_7s^5 + ae_1e_3s^3x + e_2e_6e_7x^3) = 0, \quad (\text{B.10})$$

⁹Were we to only use the sequence of blowups described in (4.5) and (4.6) without the additional (4.7) one would not be able to invert the equations for E_i in terms of the D_i .

where the relative projective coordinates are

$$\begin{aligned} [e_2 e_4 e_5 e_6 e_7^2 x : e_2 e_3 e_4^2 e_5^3 e_6^2 e_7^4 y : s] [x : e_3 e_4 e_5^2 e_6 e_7^2 y : e_1 e_3 e_4 e_5 e_7] \\ [e_5 e_6 e_7 y : e_1] [e_2 e_6 e_7 : e_3] [e_6 y : e_4] [y : e_2 e_7] [e_2 : e_5]. \end{aligned} \quad (\text{B.11})$$

The total transform of s is $se_1 e_2 e_3 e_4^2 e_5^2 e_6 e_7^3$ and we have the following fibral divisors

$$\begin{cases} 1 D_0 : & s = e_3 e_5 e_6 y^2 - e_1 e_2^2 e_4 e_6 e_7 x^3 = 0, \\ 2 D_1 : & e_1 = e_3 = 0, \\ 3 D_2 : & e_3 = e_4 = 0, \\ 4 D_3 : & e_4 = e_5 = 0, \\ 3 D_4 : & e_7 = e_5 e_6 y^2 - a e_1^2 e_2 e_4 s^3 x = 0, \\ 2 D_5 : & e_2 = e_6 = 0, \\ 1 D_6 : & e_6 = b e_1 e_3 e_4 e_5 e_7 s^2 + a x = 0, \\ 2 D_7 : & e_5 = a e_1 e_3 s^3 + e_2 e_6 e_7 x^2 = 0. \end{cases} \quad (\text{B.12})$$

The classes of the Cartier divisors defined by the zero loci of the variables s, x, y, e_i are

$$\begin{cases} [s] = S - E_1, & [x] = H + 2L - E_1 - E_2, & [y] = H + 3L - E_1 - E_2 - E_3 - E_5 - E_6, \\ [e_1] = E_1 - E_2 - E_3, & [e_2] = E_2 - E_4 - E_6 - E_7, & [e_3] = E_3 - E_4, \\ [e_4] = E_4 - E_5, & [e_5] = E_5 - E_7, & [e_6] = E_6, & [e_7] = E_7, \end{cases} \quad (\text{B.13})$$

where E_i is the total transform of the i^{th} exceptional divisor and $[e_i]$ is the proper transform of the i^{th} exceptional divisor.

We have the linear relations

$$\begin{aligned} [e_1] = D_1, \quad [e_2] = D_5, \quad [e_3] = D_1 + D_2, \quad [e_4] = D_2 + D_3, \\ [e_5] = D_3 + D_7, \quad [e_6] = D_5 + D_6, \quad [e_7] = D_4, \end{aligned} \quad (\text{B.14})$$

and can thus solve for the D_i in terms of the E_i to get

$$\begin{cases} D_0 = S - E_1, \\ D_1 = E_1 - E_2 - E_3, \\ D_2 = -E_1 + E_2 + 2E_3 - E_4, \\ D_3 = E_1 - E_2 - 2E_3 + 2E_4 - E_5, \\ D_4 = E_7, \\ D_5 = E_2 - E_4 - E_6 - E_7, \\ D_6 = -E_2 + E_4 + 2E_6 + E_7, \\ D_7 = -E_1 + E_2 + 2E_3 - 2E_4 + 2E_5 - E_7. \end{cases} \quad (\text{B.15})$$

Now that we have the classes of the fibral divisors, the sequence of blowups and the pushforward

theorems will be enough to compute the triple intersection numbers. Noting that

$$[Y_5] = 3H + 6L - 2E_1 - 2E_2 - E_3 - E_4 - E_5 - E_6 - E_7, \quad (\text{B.16})$$

we can use the pushforward theorems from Section 5 to get:

$$\begin{aligned} F_5(\phi) = & 4S(L - S)(\phi_0^3 + \phi_1^3 + \phi_2^3 + \phi_3^3 + \phi_5^3) - S^2(\phi_4^3 + \phi_6^3 + \phi_7^3) \\ & + 3S(3S - 4L)(\phi_3\phi_2^2 - \phi_3\phi_4^2 + \phi_4\phi_6^2 + \phi_4\phi_7^2 + \phi_6\phi_7^2 + \phi_4^2\phi_6 + \phi_6^2\phi_7 - \phi_3\phi_7^2 + \phi_7\phi_4^2) \\ & + 3S\phi_1\phi_0^2(S - 2L) + 3LS\phi_1^2\phi_0 + 3S(3L - 2S)(\phi_2\phi_3^2 - \phi_1^2\phi_2) \\ & + 3S(5L - 4S)(2\phi_5\phi_6^2 - \phi_3^2\phi_4 - \phi_3^2\phi_7) + 3S(2L - S)\phi_1\phi_2^2 + 3S(9S - 11L)\phi_5^2\phi_6 \\ & + 3S(S - L)(2\phi_4^2\phi_5 - \phi_4\phi_5^2) + 6S(4L - 3S)(\phi_4\phi_5\phi_6 + \phi_3\phi_4\phi_7 + \phi_4\phi_6\phi_7). \end{aligned} \quad (\text{B.17})$$

B.3 Y_6

Y_6 is the proper transform of the Weierstrass model of equation (2.2) after the blowups leading to X_7^- in (4.1). The result is

$$Y_6 : \quad e_3e_5e_6y^2 - e_1e_2e_4(be_1^2e_3^2e_4e_5s^5 + ae_1e_3s^3x + e_2e_6e_7^2x^3) = 0, \quad (\text{B.18})$$

where the relative projective coordinates are

$$\begin{aligned} [e_2e_4e_5e_6e_7^2x : e_2e_3e_4^2e_5^3e_6^2e_7^3y : s] [x : e_3e_4e_5^2e_6e_7y : e_1e_3e_4e_5] \\ [e_5e_6e_7y : e_1] [e_2e_6e_7^2 : e_3] [e_6e_7y : e_4] [y : e_2e_7] [e_2 : e_6]. \end{aligned} \quad (\text{B.19})$$

The total transform of s is $se_1e_2e_3e_4^2e_5^2e_6e_7^2$ and we have the following fibral divisors

$$\left\{ \begin{array}{l} 1 D_0 : \quad s = e_3e_5y^2 - e_1e_2^2e_4e_7^2x^3 = 0, \\ 2 D_1 : \quad e_1 = e_3 = 0, \\ 3 D_2 : \quad e_3 = e_4 = 0, \\ 4 D_3 : \quad e_4 = e_5 = 0, \\ 3 D_4 : \quad e_2 = e_5 = 0, \\ 2 D_5 : \quad e_7 = e_5e_6y^2 - ae_1^2e_2e_4s^3x - be_1^3e_2e_3e_4^2e_5s^5 = 0, \\ 1 D_6 : \quad e_6 = be_1e_3e_4e_5s^2 + ax = 0, \\ 2 D_7 : \quad e_5 = ae_1e_3s^3 + e_2e_6e_7^2x^2 = 0. \end{array} \right. \quad (\text{B.20})$$

The classes of the Cartier divisors defined by the zero loci of the variables s, x, y, e_i are

$$\left\{ \begin{array}{l} [s] = S - E_1, \quad [x] = H + 2L - E_1 - E_2, \quad [y] = H + 3L - E_1 - E_2 - E_3 - E_5 - E_6, \\ [e_1] = E_1 - E_2 - E_3, \quad [e_2] = E_2 - E_4 - E_6 - E_7, \quad [e_3] = E_3 - E_4, \\ [e_4] = E_4 - E_5, \quad [e_5] = E_5, \quad [e_6] = E_6 - E_7, \quad [e_7] = E_7, \end{array} \right. \quad (\text{B.21})$$

where E_i is the total transform of the i^{th} exceptional divisor and $[e_i]$ is the proper transform of the i^{th} exceptional divisor.

We have the linear relations

$$\begin{aligned} [e_1] &= D_1, & [e_2] &= D_4, & [e_3] &= D_1 + D_2, & [e_4] &= D_2 + D_3, \\ [e_5] &= D_3 + D_4 + D_7, & [e_6] &= D_6, & [e_7] &= D_5, \end{aligned} \quad (\text{B.22})$$

and can thus solve for the D_i in terms of the E_i to get

$$\begin{cases} [D_0] &= S - E_1, \\ [D_1] &= E_1 - E_2 - E_3, \\ [D_2] &= -E_1 + E_2 + 2E_3 - E_4, \\ [D_3] &= E_1 - E_2 - 2E_3 + 2E_4 - E_5, \\ [D_4] &= E_2 - E_4 - E_6 - E_7, \\ [D_5] &= E_7, \\ [D_6] &= E_6 - E_7, \\ [D_7] &= -E_1 + 2E_3 - E_4 + 2E_5 + E_6 + E_7. \end{cases} \quad (\text{B.23})$$

Now that we have the classes of the fibral divisors, the sequence of blowups and the pushforward theorems will be enough to compute the triple intersection numbers. Noting that

$$[Y_6] = 3H + 6L - 2E_1 - 2E_2 - E_3 - E_4 - E_5 - E_6 - E_7, \quad (\text{B.24})$$

we can use the pushforward theorems from Section 5 to get:

$$\begin{aligned} F_6(\phi) &= 4S(L - S)(\phi_0^3 + \phi_1^3 + \phi_2^3 + \phi_3^3 + \phi_4^3 + \phi_6^3) - S^2\phi_5^3 - 2S(2L - S)\phi_7^3 \\ &\quad + 6S(4L - 3S)(\phi_3\phi_4\phi_7 + \phi_4\phi_5\phi_7 + \phi_5\phi_6\phi_7) + 3LS\phi_0\phi_1^2 \\ &\quad + 3S(3S - 4L)(\phi_3\phi_2^2 - \phi_3\phi_4^2 - \phi_3\phi_7^2 + \phi_5\phi_7^2 + 2\phi_4^2\phi_7 + \phi_5^2\phi_7 + 2\phi_6^2\phi_7) \\ &\quad + 3S(S - 2L)(\phi_1\phi_0^2 - \phi_1\phi_2^2) + 3S(3L - 2S)(\phi_2\phi_3^2 - \phi_1^2\phi_2) + 3S(6S - 7L)\phi_5^2\phi_6 \\ &\quad + 3S(5L - 4S)(\phi_4\phi_5^2 - \phi_3^2\phi_7 - \phi_3^2\phi_4) + 3S(6L - 5S)(\phi_5\phi_6^2 - \phi_4^2\phi_5). \end{aligned} \quad (\text{B.25})$$

B.4 Y_8

Y_8 is the proper transform of the Weierstrass model of equation (2.2) after the blowups leading to X'_7 in (4.1). The result is

$$Y_8 : \quad e_3e_5e_7y^2 - e_1e_2e_4(be_1^2e_3^2e_4e_5e_6s^5 + ae_1e_3s^3x + e_2e_6e_7x^3) = 0, \quad (\text{B.26})$$

where the relative projective coordinates are

$$\begin{aligned} [e_2e_4e_5e_6^2e_7x : e_2e_3e_4^2e_5^3e_6^4e_7^2y : s] & [x : e_3e_4e_5^2e_6^2e_7y : e_1e_3e_4e_5e_6] \\ [e_5e_6e_7y : e_1] & [e_2e_6e_7 : e_3] [e_7y : e_4] [e_2e_7 : e_5] [y : e_2]. \end{aligned} \quad (\text{B.27})$$

The total transform of s is $se_1e_2e_3e_4^2e_5^2e_6^3e_7$ and we have the following fibral divisors

$$\left\{ \begin{array}{l} 1 D_0 : \quad s = e_3e_5y^2 - e_1e_2^2e_4e_6x^3 = 0, \\ 2 D_1 : \quad e_1 = e_3 = 0, \\ 3 D_2 : \quad e_3 = e_4 = 0, \\ 4 D_3 : \quad e_4 = e_5 = 0, \\ 3 D_4 : \quad e_6 = e_5e_7y^2 - ae_1^2e_2e_4s^3x = 0, \\ 2 D_5 : \quad e_2 = e_7 = 0, \\ 1 D_6 : \quad e_7 = be_1e_3e_4e_5e_6s^2 + ax = 0, \\ 2 D_7 : \quad e_5 = ae_1e_3s^3 + e_2e_6e_7x^2 = 0. \end{array} \right. \quad (\text{B.28})$$

The classes of the Cartier divisors defined by the zero loci of the variables s, x, y, e_i are

$$\left\{ \begin{array}{l} [s] = S - E_1, \quad [x] = H + 2L - E_1 - E_2, \quad [y] = H + 3L - E_1 - E_2 - E_3 - E_5 - E_7, \\ [e_1] = E_1 - E_2 - E_3, \quad [e_2] = E_2 - E_4 - E_6 - E_7, \quad [e_3] = E_3 - E_4, \\ [e_4] = E_4 - E_5, \quad [e_5] = E_5 - E_6, \quad [e_6] = E_6, \quad [e_7] = E_7, \end{array} \right. \quad (\text{B.29})$$

where E_i is the total transform of the i^{th} exceptional divisor and $[e_i]$ is the proper transform of the i^{th} exceptional divisor.

We have the linear relations

$$\begin{aligned} [e_1] &= D_1, \quad [e_2] = D_5, \quad [e_3] = D_1 + D_2, \quad [e_4] = D_2 + D_3, \\ [e_5] &= D_3 + D_7, \quad [e_6] = D_4, \quad [e_7] = D_5 + D_6, \end{aligned} \quad (\text{B.30})$$

and can thus solve for the D_i in terms of the E_i to get

$$\left\{ \begin{array}{l} [D_0] = S - E_1, \\ [D_1] = E_1 - E_2 - E_3, \\ [D_2] = -E_1 + E_2 + 2E_3 - E_4, \\ [D_3] = E_1 - E_2 - 2E_3 + 2E_4 - E_5, \\ [D_4] = E_6, \\ [D_5] = E_2 - E_4 - E_6 - E_7, \\ [D_6] = -E_2 + E_4 + E_6 + 2E_7, \\ [D_7] = -E_1 + E_2 + 2E_3 - 2E_4 + 2E_5 - E_6. \end{array} \right. \quad (\text{B.31})$$

Now that we have the classes of the fibral divisors, the sequence of blowups and the pushforward theorems will be enough to compute the triple intersection numbers. Noting that

$$[Y_8] = 3H + 6L - 2E_1 - 2E_2 - E_3 - E_4 - E_5 - E_6 - E_7, \quad (\text{B.32})$$

we can use the pushforward theorems from Section 5 to get:

$$\begin{aligned}
F_8(\phi) = & 4S(L - S)\phi_0^3 + 3LS\phi_0\phi_1^2 + 3S(S - 2L)\phi_0^2\phi_1 \\
& + 4S(L - S)(\phi_1^3 + \phi_2^3 + \phi_3^3 + \phi_5^3 + \phi_6^3 + \phi_7^3) + 2S(S - 2L)\phi_4^3 \\
& + 3S(2L - S)\phi_1\phi_2^2 + 3S(2S - 3L)\phi_1^2\phi_2 + 3S(3L - 2S)\phi_2\phi_3^2 + 3S(3S - 4L)\phi_2^2\phi_3 \\
& + 6S(5L - 4S)\phi_5\phi_6^2 + 3S(9S - 11L)\phi_5^2\phi_6 + 3S(4S - 5L)\phi_3^2\phi_7 \\
& + 3S(L - S)\phi_4\phi_5^2 + 3S(4S - 5L)\phi_3^2\phi_4 + 6S(S - L)\phi_4^2\phi_5 \\
& + 6S(3S - 4L)\phi_4(\phi_6^2 - \phi_5\phi_6 + \phi_7^2) + 3S(4L - 3S)\phi_3(\phi_4 + \phi_7)^2.
\end{aligned} \tag{B.33}$$

Now that we have the triple intersection polynomial for each chamber, we conclude this appendix with a brief discussion of how to use this data to learn about the geometry of the fibral divisors. In particular, a necessary condition for a divisor D_i to be a \mathbb{P}^1 -bundle without singular fibers is that

$$D_i^3 = 4S(L - S). \tag{B.34}$$

By looking at the Fermat terms of the triple intersection polynomials F_8 , F_6 , F_5 , and F_4 , we see that we recover the following information:

1. In Ch_4 , D_3 and D_6 are not \mathbb{P}^1 -bundles.
2. In Ch_5 , D_4 , D_6 , and D_7 are not \mathbb{P}^1 -bundles.
3. In Ch_6 , D_5 and D_7 are not \mathbb{P}^1 -bundles.
4. In Ch_8 , D_4 is not a \mathbb{P}^1 -bundle.

We note that these conclusions are consistent with the analysis in [25].

For example, in chamber 8, since the divisors D_a for $a = 0, 1, 2, 3, 5, 6, 7$ have fibers that do not degenerate, they are projective bundles. We can check that their triple intersection numbers are as expected:

$$D_0^3 = D_1^3 = D_2^3 = D_3^3 = D_5^3 = D_6^3 = D_7^3 = 4(L - S)S. \tag{B.35}$$

The divisor D_4 has a fiber that degenerates with the appearance of two new curves over $V(a, s)$. This is also reflected in its triple intersection:

$$D_4^3 = 2S(-2L + S), \tag{B.36}$$

which differs from that of a projective bundle over S by 2 for each point of $V(a, s)$:

$$D_4^3 = 4(L - S)S - 2(4L - 3S)S = 4(L - S)S - 2[a] \cdot S, \tag{B.37}$$

where we used

$$(4L - 3S)S = [a] \cdot [s]. \tag{B.38}$$

We see D_4 has the same self-triple intersection as a projective bundle with $2[a] \cdot S$ points blown-up.

C Fibral divisors from scaling

In this appendix, we demonstrate an alternate route to Table 3 via scaling methods, using D_3 as an example. The fibral divisor D_3 is not a projective bundle for Y_4 since there the curve C_3 can degenerate in codimension-two. For Y_5 , Y_6 , and Y_8 , the fibral divisor D_3 is the same \mathbb{P}^1 -bundle up to isomorphism and we will now determine its isomorphism class. It is enough to focus on the first 5 blowups these varieties have in common. Our divisor is defined by

$$D_3 : e_4 = e_5 = 0, \tag{C.1}$$

and on this locus, we have the coordinates

$$[0 : 0 : \ell_1 s] [\ell_1 \ell_2 x : 0 : 0] [0 : \ell_1^{-1} \ell_2 \ell_3 e_1] [\ell_2^{-1} \ell_4 e_2 : \ell_4 \ell_3^{-1} e_3] [\ell_1 \ell_2 \ell_3 \ell_5 y : 0], \tag{C.2}$$

where we have included the relevant rescaling factors.

	s	x	y	e_1	e_2	e_3	e_4	e_5
ℓ_1	1	1	1	-1	0	0	0	0
ℓ_2	0	1	1	1	-1	0	0	0
ℓ_3	0	0	1	1	0	-1	0	0
ℓ_4	0	0	0	0	1	1	-1	0
ℓ_5	0	0	1	0	0	0	1	-1

(C.3)

We recall that the components of a given set of projective coordinates cannot be simultaneously zero. Thus, the fibral divisor D_3 is defined in the patch

$$sxye_1 \neq 0. \tag{C.4}$$

To normalize the coordinates $[0 : 0 : s][x : 0 : 0][0 : e_1][y : 0]$ to $[0 : 0 : 1][1 : 0 : 0][0 : 1][1 : 0]$, we take

$$\ell_1 = s^{-1}, \quad \ell_2 = sx^{-1}, \quad \ell_3 = e_1^{-1}s^{-2}x, \quad \ell_5 = e_1s^2y^{-1}. \tag{C.5}$$

This implies that the fiber is

$$\left[e_2 \frac{x}{s} : e_1 e_3 \frac{s^2}{x} \right] \cong [e_2 x^2 : e_1 e_3 s^3], \tag{C.6}$$

and we deduce that

$$D_3 \cong \mathbb{P}_S(\mathcal{S}^{\otimes 3} \oplus \mathcal{L}^{\otimes 4}), \tag{C.7}$$

which agrees with the corresponding entries in Table 3.

D Vertical rational surfaces

In this appendix, we prove Theorem 8.1 by analyzing the isomorphism class of the curve C_6 over the locus $V(a, b) \cap S$. This requires a careful analysis of the projective space defined from X_0 by the sequence of blowups.

D.1 The vertical surface Q_8

In the case of Y_8 , the defining equation for C_6 is

$$C_6 : e_7 = be_1e_3e_4e_5e_6s^2 + ax = 0. \quad (D.1)$$

The projective coordinates of the fiber of X_7 over X_0 are:

$$[0 : 0 : s][x : 0 : e_1e_3e_4e_5e_6][0 : e_1][0 : e_3][0 : e_4][0 : e_5][y : e_2], \quad (D.2)$$

which shows C_6 is defined in the open patch

$$se_1e_3e_4e_5 \neq 0. \quad (D.3)$$

The scaling symmetries due to the respective blowups from X_0 to X'_7 are:

X'_7	s	x	y	e_1	e_2	e_3	e_4	e_5	e_6	e_7
l_1	1	1	1	-1	0	0	0	0	0	0
l_2	0	1	1	1	-1	0	0	0	0	0
l_3	0	0	1	1	0	-1	0	0	0	0
l_4	0	0	0	0	1	1	-1	0	0	0
l_5	0	0	1	0	0	0	1	-1	0	0
l_6	0	0	0	0	1	0	0	1	-1	0
l_7	0	0	1	0	1	0	0	0	0	-1

(D.4)

We introduce the following linear redefinitions:

X'_7	s	x	y	e_1	e_2	e_3	e_4	e_5	e_6	e_7
$l'_1 = l_1 + l_3 + l_4 + l_5 + l_6$	1	1	3	0	2	0	0	0	-1	0
$l'_2 = l_2 - l_3 - l_4 - l_5 - l_6 + 3l_7$	0	1	2	0	0	0	0	0	1	-3
$l'_3 = l_3 + l_4 + l_5 + l_6$	0	0	2	1	2	0	0	0	-1	0
$l'_4 = l_4 + l_5 + l_6$	0	0	1	0	2	1	0	0	-1	0
$l'_5 = l_5 + l_6$	0	0	1	0	1	0	1	0	-1	0
$l'_6 = l_6$	0	0	0	0	1	0	0	1	-1	0
$l'_7 = l_7$	0	0	1	0	1	0	0	0	0	-1

(D.5)

We fix (s, e_1, e_3, e_4, e_5) by using $(l'_1, l'_3, l'_4, l'_5, l'_6)$, respectively. Then, after imposing $e_7 = 0$, we are left with:

Q_8	x	y	e_2	e_6
$l'_2 = l_2 - l_3 - l_4 - l_5 - l_6 + 3l_7$	1	2	0	1
$l'_7 = l_7$	0	1	1	0

(D.6)

which is the toric description of the Hirzebruch surface \mathbb{F}_2 .

D.2 The vertical surface Q_6

In the case of Y_6 , the defining equation for C_6 is

$$C_6 : e_6 = be_1e_3e_4e_5s^2 + ax = 0. \quad (D.7)$$

Imposing $e_6 = 0$ gives the following projective coordinates

$$[0 : 0 : s] [x : 0 : e_1e_3e_4e_5] [0 : e_1] [0 : e_3] [0 : e_4] [y : e_2e_7] [e_2 : 0], \quad (D.8)$$

which implies that

$$se_1e_2e_3e_4 \neq 0. \quad (D.9)$$

The defining equation of C_6 gives a full rational surface Q_6 when $a = b = 0$. The successive blowups that produced X_7^- give the following scalings:

X_7^-	s	x	y	e_1	e_2	e_3	e_4	e_5	e_6	e_7
l_1	1	1	1	-1	0	0	0	0	0	0
l_2	0	1	1	1	-1	0	0	0	0	0
l_3	0	0	1	1	0	-1	0	0	0	0
l_4	0	0	0	0	1	1	-1	0	0	0
l_5	0	0	1	0	0	0	1	-1	0	0
l_6	0	0	1	0	1	0	0	0	-1	0
l_7	0	0	0	0	1	0	0	0	1	-1

(D.10)

We conveniently redefined them as follows:

X_7^-	s	x	y	e_1	e_2	e_3	e_4	e_5	e_6	e_7
$l_1 + l_3 + l_4 + l_5 - l_6$	1	1	2	0	0	0	0	-1	1	0
$l_2 - l_3 - l_4 - l_5 + l_7$	0	1	-1	0	-1	0	0	1	1	-1
$l_3 + l_4 + l_5 - l_6$	0	0	1	1	0	0	0	-1	1	0
$l_4 + l_5 - l_6$	0	0	0	0	0	1	0	-1	1	0
$l_5 - l_6 + l_7$	0	0	0	0	0	0	1	-1	2	-1
$l_2 - l_3 - l_4 - l_5 + 2l_6$	0	1	1	0	0	0	0	1	-2	0
$l_6 - l_7$	0	0	1	0	0	0	0	0	-2	1

(D.11)

We can then fix (s, e_1, e_2, e_3, e_4) by using $(l'_1, l'_2, l'_3, l'_4, l'_5)$, respectively, and after imposing $e_6 = 0$, we are left with:

Q_6	x	y	e_5	e_7
$l'_6 = l_2 - l_3 - l_4 - l_5 + 2l_6$	1	1	1	0
$l'_7 = l_6 - l_7$	0	1	0	1

(D.12)

which shows that Q_6 is isomorphic to a Hirzebruch surface F_1 .

D.3 The vertical surface Q_5

The surface Q_5 is defined by

$$C_6 : e_6 = be_1e_3e_4e_5e_7s^2 + ax = 0, \quad (D.13)$$

which reduces to $e_6 = 0$ over $V(a, b) \cap S$ in Y_5 . The projective coordinates are:

$$[0 : 0 : s] [x : 0 : e_1e_3e_4e_5e_7][0 : e_1] [0 : e_3] [0 : e_4] [y : e_2e_7] [e_2 : e_5], \quad (D.14)$$

which imply that

$$se_1e_3e_4 \neq 0. \quad (D.15)$$

The successive blowups defining X_7^+ give the scalings:

X_7^+	s	x	y	e_1	e_2	e_3	e_4	e_5	e_6	e_7
l_1	1	1	1	-1	0	0	0	0	0	0
l_2	0	1	1	1	-1	0	0	0	0	0
l_3	0	0	1	1	0	-1	0	0	0	0
l_4	0	0	0	0	1	1	-1	0	0	0
l_5	0	0	1	0	0	0	1	-1	0	0
l_6	0	0	1	0	1	0	0	0	-1	0
l_6	0	0	0	0	1	0	0	1	0	-1

(D.16)

which we redefine as follows:

X_7^+	s	x	y	e_1	e_2	e_3	e_4	e_5	e_6	e_7
$l'_1 = l_1 + l_3 + l_4 + l_5 - l_6$	1	1	2	0	0	0	0	-1	1	0
$l'_2 = l_2 - l_3 - l_4 - l_5 + 2l_6$	0	1	1	0	0	0	0	1	-2	0
$l'_3 = l_3 + l_4 + l_5 - l_6$	0	0	1	1	0	0	0	-1	1	0
$l'_4 = l_4 + l_5 - l_6$	0	0	0	0	0	1	0	-1	1	0
$l'_5 = l_5 - l_6 + l_7$	0	0	0	0	0	0	1	0	1	-1
$l'_6 = l_6$	0	0	1	0	1	0	0	0	-1	0
$l'_7 = l_7$	0	0	0	0	1	0	0	1	0	-1

(D.17)

We can then fix (s, e_1, e_3, e_4) using (l'_1, l'_3, l'_4, l'_5) . After imposing $e_6 = 0$, we are left with:

Q_5	x	y	e_2	e_5	e_7
$l'_2 = l_2 - l_3 - l_4 - l_5 + 2l_6$	1	1	0	1	0
$l'_6 = l_6$	0	1	1	0	0
$l'_7 = l_7$	0	0	1	1	-1

(D.18)

which shows that Q_5 is a Hirzebruch surface \mathbb{F}_1 blown-up at a point (namely $e_2 = e_5 = 0$) of its unique curve of self-intersection -1 .

D.4 The vertical surface Q_4

The surface Q_4 is defined by

$$C_6 : e_5 = be_1e_3e_4e_6e_7^2s^2 + ax = 0, \quad (D.19)$$

which reduces to $e_5 = 0$ over $V(a, b) \cap S$. The projective coordinates are

$$[0 : 0 : s] [x : 0 : e_1e_3e_4e_6e_7^2] [0 : e_1] [0 : e_3] [e_6e_7y : e_2] [y : e_4e_7] [e_4 : e_6], \quad (D.20)$$

which means that we have

$$se_1e_3 \neq 0. \quad (D.21)$$

The successive blowups defining X_7'' give the scalings:

X_7''	s	x	y	e_1	e_2	e_3	e_4	e_5	e_6	e_7
ℓ_1	1	1	1	-1	0	0	0	0	0	0
ℓ_2	0	1	1	1	-1	0	0	0	0	0
ℓ_3	0	0	1	1	0	-1	0	0	0	0
ℓ_4	0	0	0	0	1	1	-1	0	0	0
ℓ_5	0	0	1	0	1	0	0	-1	0	0
ℓ_6	0	0	1	0	0	0	1	0	-1	0
ℓ_7	0	0	0	0	0	0	1	0	1	-1

(D.22)

We redefine them as follows:

X_7''	s	x	y	e_1	e_2	e_3	e_4	e_5	e_6	e_7
$\ell'_1 = \ell_1 + \ell_2$	1	2	2	0	-1	0	0	0	0	0
$\ell'_2 = \ell_2 - \ell_3 - \ell_4 + 2\ell_5$	0	1	2	0	0	0	1	-2	0	0
$\ell'_3 = \ell_3 + \ell_4$	0	0	1	1	1	0	-1	0	0	0
$\ell'_4 = \ell_4$	0	0	0	0	1	1	-1	0	0	0
$\ell'_5 = \ell_5$	0	0	1	0	1	0	0	-1	0	0
$\ell'_6 = \ell_6$	0	0	1	0	0	0	1	0	-1	0
$\ell'_7 = \ell_7$	0	0	0	0	0	0	1	0	1	-1

(D.23)

which allows us to fix (s, e_1, e_3) using $(\ell'_1, \ell'_2, \ell'_3)$. After imposing $e_5 = 0$, we are left with:

Q_4	x	y	e_2	e_4	e_6	e_7
$\ell'_2 = \ell_2 - \ell_3 - \ell_4 + 2\ell_5$	1	2	0	1	0	0
$\ell'_5 = \ell_5$	0	1	1	0	0	0
$\ell'_6 = \ell_6$	0	1	0	1	-1	0
$\ell'_7 = \ell_7$	0	0	0	1	1	-1

(D.24)

which is a Hirzebruch surface \mathbb{F}_2 (parametrized by (x, y, e_2, e_4)), blown-up at a point $P : y = e_4 = 0$ of its curve of self-intersection 2, followed by a blowup of the intersection point $(e_4 = e_5 = 0)$ of the resulting exceptional fiber and the proper transform of the fiber over the point P .

Acknowledgements

M.E. is supported in part by the National Science Foundation (NSF) grant DMS-1701635 “Elliptic Fibrations and String Theory.” We would like to thank Patrick Jefferson and Monica Jinwoo Kang for conversations.

References

- [1] P. Aluffi. Chern classes of blow-ups. *Math. Proc. Cambridge Philos. Soc.*, 148(2):227–242, 2010.
- [2] P. Aluffi and M. Esole. Chern class identities from tadpole matching in type IIB and F-theory. *JHEP*, 03:032, 2009.
- [3] P. Aluffi and M. Esole. New Orientifold Weak Coupling Limits in F-theory. *JHEP*, 02:020, 2010.
- [4] P. S. Aspinwall and M. Gross, “The $SO(32)$ heterotic string on a K3 surface,” *Phys. Lett. B* **387**, 735 (1996) doi:10.1016/0370-2693(96)01095-7 [hep-th/9605131].
- [5] P. S. Aspinwall, S. H. Katz and D. R. Morrison, “Lie groups, Calabi-Yau threefolds, and F theory,” *Adv. Theor. Math. Phys.* **4**, 95 (2000) [hep-th/0002012].
- [6] L. Bhardwaj and P. Jefferson, “Classifying 5d SCFTs via 6d SCFTs: Rank one,” arXiv:1809.01650 [hep-th].
- [7] M. Bershadsky, K. A. Intriligator, S. Kachru, D. R. Morrison, V. Sadov, and C. Vafa. Geometric singularities and enhanced gauge symmetries. *Nucl. Phys.*, B481:215–252, 1996.
- [8] R. Borcherds. Lie Groups. <https://math.berkeley.edu/~reb/courses/261/all.pdf> (updated May 25, 2012).
- [9] N. Bourbaki, *Groups and Lie Algebras. Chap. 4–6*, Translated from the 1968 French original. Elements of Mathematics (Berlin). Springer-Verlag, Berlin Heidelberg, 2002.
- [10] P. Candelas, D. E. Diaconescu, B. Florea, D. R. Morrison and G. Rajesh, “Codimension three bundle singularities in F theory,” *JHEP* **0206**, 014 (2002) doi:10.1088/1126-6708/2002/06/014 [hep-th/0009228].
- [11] M. Del Zotto, J. J. Heckman and D. R. Morrison, “6D SCFTs and Phases of 5D Theories,” arXiv:1703.02981 [hep-th].
- [12] D. E. Diaconescu and R. Entin, “Calabi-Yau spaces and five-dimensional field theories with exceptional gauge symmetry,” *Nucl. Phys. B* **538**, 451 (1999) doi:10.1016/S0550-3213(98)00689-0 [hep-th/9807170].
- [13] M. Esole, “Introduction to Elliptic Fibrations,” doi:10.1007/978-3-319-65427-07.
- [14] M. Esole, S. G. Jackson, R. Jagadeesan, and A. G. Noël, “Incidence Geometry in a Weyl Chamber I: GL_n ,” arXiv:1508.03038 [math.RT].

- [15] M. Esole, S. G. Jackson, R. Jagadeesan, and A. G. Noël, “Incidence Geometry in a Weyl Chamber II: SL_n ,” arXiv:1601.05070 [math.RT].
- [16] M. Esole, R. Jagadeesan and M. J. Kang, “The Geometry of G_2 , Spin(7), and Spin(8)-models,” arXiv:1709.04913 [hep-th].
- [17] M. Esole, P. Jefferson and M. J. Kang, “The Geometry of F_4 -Models,” arXiv:1704.08251 [hep-th].
- [18] M. Esole, P. Jefferson and M. J. Kang, “Euler Characteristics of Crepant Resolutions of Weierstrass Models,” Commun. Math. Phys. **371** (2019) no.1, 99-144 doi:10.1007/s00220-019-03517-1 [arXiv:1703.00905 [math.AG]].
- [19] M. Esole and M. J. Kang, “Characteristic numbers of elliptic fibrations with non-trivial Mordell-Weil groups,” [arXiv:1808.07054 [hep-th]].
- [20] M. Esole and M. J. Kang, “Characteristic numbers of crepant resolutions of Weierstrass models,” arXiv:1807.08755 [hep-th].
- [21] M. Esole and M. J. Kang, “The Geometry of the $SU(2) \times G_2$ -model,” arXiv:1805.03214 [hep-th].
- [22] M. Esole and M. J. Kang, “Flopping and slicing: $SO(4)$ and Spin(4)-models,” Adv. Theor. Math. Phys. **23** (2019) no.4, 1003-1066 doi:10.4310/ATMP.2019.v23.n4.a2 [arXiv:1802.04802 [hep-th]].
- [23] M. Esole, M. J. Kang and S. T. Yau, “Mordell-Weil Torsion, Anomalies, and Phase Transitions,” arXiv:1712.02337 [hep-th].
- [24] M. Esole, M. J. Kang, and S.-T. Yau, “A New Model for Elliptic Fibrations with a Rank One Mordell-Weil Group: I. Singular Fibers and Semi-Stable Degenerations,” 2014.
- [25] M. Esole and S. Pasterski, “ D_4 -flops of the E_7 -model,” arXiv:1901.00093 [hep-th].
- [26] J. Fullwood. On generalized Sethi-Vafa-Witten formulas. *J. Math. Phys.*, 52:082304, 2011.
- [27] H. Hayashi, C. Lawrie, D. R. Morrison, and S. Schafer-Nameki. Box Graphs and Singular Fibers. *JHEP*, 1405:048, 2014.
- [28] K. A. Intriligator, D. R. Morrison, and N. Seiberg. Five-dimensional supersymmetric gauge theories and degenerations of Calabi-Yau spaces. *Nucl.Phys.*, B497:56–100, 1997.
- [29] S. Katz, D. R. Morrison, S. Schafer-Nameki, and J. Sully. Tate’s algorithm and F-theory. *JHEP*, 1108:094, 2011.
- [30] Y. Kawamata. Flops Connect Minimal Models. *Publ. Res. Inst. Math. Sci.* 44 (2008), 419-423.
- [31] K. Kodaira. On compact analytic surfaces. II, III. *Ann. of Math. (2)* 77 (1963), 563–626; *ibid.*, 78:1–40, 1963.
- [32] J. Kollár and S. Mori, *Birational Geometry of Algebraic Varieties*, Cambridge Univ. Press, Cambridge, 1998.

- [33] C. Lawrie and S. Schäfer-Nameki, The Tate Form on Steroids: Resolution and Higher Codimension Fibers, *JHEP* **1304**, 061 (2013).
- [34] J. M. Maldacena, A. Strominger and E. Witten, Black hole entropy in M theory, *JHEP* **9712**, 002 (1997).
- [35] K. Matsuki, Introduction to the Mori Program. Springer Science & Business Media, 2013.
- [36] A. Néron. Modèles minimaux des variétés abéliennes sur les corps locaux et globaux. *Inst. Hautes Études Sci. Publ.Math. No.*, 21:128, 1964.
- [37] K. Oguiso and T. Peternell, Calabi–Yau threefolds with positive second Chern class, *Comm. Anal. Geom.* 6 (1998) 153-172.
- [38] J. Tate. Algorithm for determining the type of a singular fiber in an elliptic pencil. In *Modular functions of one variable, IV (Proc. Internat. Summer School, Univ. Antwerp, Antwerp, 1972)*, pages 33–52. Lecture Notes in Math., Vol. 476. Springer, Berlin, 1975.
- [39] P.M.H. Wilson, The Kähler Cone on Calabi–Yau threefolds, *Invent. math.* 107 (1992) 561-583. Erratum, *Invent. math.* 114 (1993) 231-233.